Characterization of toxin-producing strains of Dinophysis spp. (Dinophyceae) isolated from French coastal waters, with a particular focus on the D. acuminata-complex

Veronique Séchet, Manoella Sibat, Gwenael Bilien, Liliane Carpentier, Georges-Augustin Rovillon, Virginie Raimbault, Florent Malo, Sylvain Gaillard, Myriam Perrière-Rumebe, Philipp Hess, et al.

Characterization of toxin-producing strains of *Dinophysis* spp. (Dinophyceae) isolated from French coastal waters, with a particular focus on the *D. acuminata*-complex.

Véronique Séchet[*1], Manoella Sibat[1], Gwenael Billien[2], Liliane Carpentier[1], Georges-Augustin Rovillon[1], Virginie Raimbault[1], Florent Malo[1], Sylvain Gaillard[1], Myriam Perrière-Rumebe[3], Philipp Hess[1], Nicolas Chomérat[2].

[1]Ifremer, DYNECO, Laboratoire Phycotoxines, F-44000 Nantes, France,

[2]Ifremer, LITTORAL, Laboratoire Environnement Ressources de Bretagne Occidentale, Station de Biologie Marine de Concarneau, 29900 Concarneau, France,

[3]Ifremer, LITTORAL, Laboratoire Environnement Ressources, 33120 Arcachon, France.

* Corresponding author: vsechet@ifremer.fr

Abstract

Dinoflagellates of the genus *Dinophysis* are the most prominent producers of Diarrhetic Shellfish Poisoning (DSP) toxins which have an impact on public health and on marine aquaculture worldwide. In particular, *Dinophysis acuminata* has been reported as the major DSP agent in Western Europe. Still, its contribution to DSP events in the regions of the English

Channel and the Atlantic coast of France, and the role of the others species of the *Dinophysis* community in these areas are not as clear. In addition, species identification within the *D. acuminata* complex has proven difficult due to their highly similar morphological features. In the present study, 30 clonal strains of the dominant *Dinophysis* species have been isolated from French coasts including the English Channel (3 sites), the Atlantic Ocean (11 sites) and the Mediterranean Sea (6 sites). Morphologically, strains were identified as three species: *D. acuta*, *D. caudata*, *D. tripos*, as well as the *D. acuminata*-complex. Sequences of the ITS and LSU rDNA regions confirmed these identifications and revealed no genetic difference within the *D. acuminata*-complex. Using the mitochondrial gene *cox1*, two groups of strains differing by only one substitution were found in the *D. acuminata*-complex, but SEM analysis of various strains showed a large range of morphological variations. Based on geographical origin and morphology, strains of the subclade A were ascribed to '*D. acuminata*' while those of the subclade B were ascribed to *D. sacculus*'. Nevertheless, the distinction into two separate species remains questionable and was not supported by our genetic data. The considerable variations observed in cultured strains suggest that physiological factors might influence cell contour and bias identification. Analyses of *Dinophysis* cultures from French coastal waters using liquid chromatography

coupled to tandem mass spectrometry (LC-MS/MS) revealed species-conserved toxin profiles for *D. acuta* (dinophysistoxin 2 (DTX2), okadaic acid (OA), pectenotoxin 2 (PTX2)), *D. caudata* (PTX2) and *D. tripos* (PTX2), irrespective of geographical origin (Atlantic Ocean or Mediterranean Sea). Within the *D. acuminata*-complex, two different toxin profiles were observed: the strains of '*D. acuminata*' (subclade A) from the English Channel and the Atlantic Ocean contained only OA while strains of *D. sacculus* (subclade B) from Mediterranean Sea/Atlantic Ocean contained PTX2 as the dominant toxin, with OA and C9-esters also being present, albeit in lower proportions. The same difference in toxin profiles between '*D. sacculus*' and '*D. acuminata*' was reported in several studies from Galicia (NW- Spain). This difference in toxin profiles has consequences in terms of public health, and consequently for monitoring programs. While toxin profile could appear as a reliable feature separating '*D. acuminata'* from '*D. sacculus'* on both French and Spanish coasts, this does not seem consistent with observations on a broader geographical scale for the *D. acuminata* complex, possibly due to the frequent lack of genetic characterization.

Highlights

► *Dinophysis* sp. has been investigated from French coastal waters using 30 monoclonal strains.

► Morphology and ITS–LSU sequences identify *D. acuta*, *D. caudata*, *D. tripos*, and *D. acuminata*-complex

► *cox1* gene reveals two subclades diverging by 1 substitution within *D. acuminata* complex

► Conserved toxin profiles in *D. acuta*, *D. caudata* and *D. tripos*, irrespective of their geographical origin.

► Two distinct toxin profiles within the *D. acuminata*-complex.

Keywords: *Dinophysis* sp., phylogeny, taxonomy, toxin profiles.

1. Introduction

Diarrhetic shellfish poisoning (DSP) events have been reported worldwide since the first documented occurrence in 1976 and 1977 along the coast of the Tohoku district in Japan which led to the identification of the dinoflagellate *Dinophysis fortii* as the toxin producer (Yasumoto et al., 1980). *Dinophysis* is one of the largest genera of dinoflagellates, with more than 200 species ascribed (Hallegraeff and Lucas, 1988), of which 133 are accepted taxonomically (Guiry, 2020). Only ten of these, as well as two species of the closely related genus *Phalacroma*, have been unambiguously reported to contain DSP toxins (MacKenzie et al., 2005; Reguera et al., 2012; Zingone and Larsen, 2020). A few hundred cells of toxic *Dinophysis* sp. per liter may suffice to generate diarrheic intoxications in humans by consuming contaminated shellfish (Yasumoto et al., 1985). *Dinophysis* species are known to produce two groups of bioactive lipophilic compounds: okadaic acid (OA) and its derivatives the dinophysistoxins (DTXs) that inhibit phosphoprotein phosphatases, are polyethers containing a carboxylic acid functionality and cause diarrhetic effects, while pectenotoxins (PTXs) are a family of polyether-lactones that are much less toxic via the oral route and do not induce diarrhea (Miles et al., 2004a).

111 During June–July 1983, at least 3300 people suffered
112 symptoms of diarrhetic shellfish poisoning (DSP) after eating
113 contaminated mussels (*Mytilus edulis*) from Southern Brittany
114 (France) before a sanitary ban was enforced (Alzieu et al., 1983).
115 This outbreak was associated with *Dinophysis acuminata* (Lassus
116 et al., 1985). Following this toxic episode the National
117 Phytoplankton and Phycotoxins Monitoring network (REPHY)
118 was set up in 1984 (Belin et al., 2020). Okadaic acid was detected
119 in contaminated mussels collected at le Havre (English Channel)
120 during a bloom of *D. acuminata* in 1984, whereas DTXs or PTXs
121 were under the limit of detection (Kumagai et al., 1986). The
122 presence of OA in bivalve molluscs collected on the English
123 channel and Atlantic coasts of France was confirmed over the
124 following years but it was noted that shellfish toxicity was not
125 always well correlated to planktonic cell concentrations
126 (Marcaillou-Le Baut and Masselin, 1989). Until the end of the
127 1990s, little attention was paid to PTXs, considered then to be a
128 toxin restricted to *D. fortii* proliferations in Japan (Reguera et al.,
129 2014). In France, the presence of PTX2 and its derivatives was
130 identified in shellfish by liquid chromatography (LC) coupled with
131 mass spectrometry (MS) analysis for the first time in 2004 in the
132 Thau lagoon on the Mediterranean coast, and in 2005 in the

Arcachon Basin on the Atlantic coast (Amzil et al., 2007). Since then, high amounts of PTX2-seco-acid have been regularly reported in the Mediterranean lagoons at sites of shellfish aquaculture (Belin and Soudant, 2018).

On the French coastline, *Dinophysis* has the particularity of rarely proliferating at high concentrations but it can be observed on all three major coastlines, i.e. the English Channel, the Atlantic and Mediterranean coasts. Maximum annual concentrations are generally below 10,000 cells·L^{-1}, however, higher *Dinophysis* concentrations have been recorded on the Normandy coast in August 2016, i.e. a maximum of 803,000 cells·L^{-1}, which is the highest value ever reached for this taxon during 30 years of the REPHY monitoring program (Belin and Soudant, 2018). In the frame of this national monitoring program, *D. acuminata* and *D. sacculus* have been identified as the dominant species at the origin of toxic episodes in the Atlantic/English Channel regions and the Mediterranean Sea, respectively, with also the more episodic or localized presence of *D. acuta*, *D. caudata, D. fortii* and *D. tripos* (Belin and Soudant, 2018). Highest concentrations of *Dinophysis acuminata* usually appear in early spring in the bay of Arcachon, subsequently (late spring - early summer) in southern Brittany, and finally in August in Normandy (English Channel)

where it can form blooms. *D. sacculus* is widely recorded in cold and temperate waters (Zingone et al., 1998), but concentrations over 1×10^3 cells·L^{-1} of this species have been only reported in warm-temperate semi-enclosed coastal areas with freshwater inputs in southwestern Europe and the Mediterranean Sea (Reguera et al., 2014). It is the dominant species in French Mediterranean lagoons but it is also observed in important aquaculture sites in western France (Belin and Soudant, 2018). Nevertheless, morphological variability due to biogeographical intra-specific differences (Zingone et al., 1998) and life cycle polymorphism (Berland et al., 1995; Nézan, 2000) resulted in uncertainty in the morphological identification and quantification of *Dinophysis* spp. natural samples. Since the often co-occurring species *D. acuminata*, *D. sacculus*, *D. ovum* and *D. pavillardii* are difficult to discriminate by morphology, the term "*D. acuminata* complex" has been introduced (Bravo et al., 1995; Lassus and Bardouil, 1991). The investigation into the morphological variability of *D. sacculus* and *D. acuminata* conducted by Zingone et al. (1998) concluded that despite the morphological variation observed in *D. sacculus* in the Mediterranean sea and along the European Atlantic coast, it could be distinguished from Atlantic populations of *D. acuminata* by small details. For instance, the shape of

hypothecal plates and curvature of the dorsal edge have been proposed to distinguish the more elongated and rectangular *D. sacculus* from the shorter and more convex *D. acuminata*. Moreover, in that study, the authors pointed out that toxic events in western France associated with *D. sacculus* need a further confirmation about the responsible species (Zingone et al., 1998).

Molecular methods have been successfully applied to identify many dinoflagellate species and clades (Penna and Magnani, 1999; Scholin and Anderson, 1996), but the genetic delineation of species within the *D. acuminata*-complex is unclear, making either ribosomal genes (SSU and LSU rDNA) or ITS regions (Edvardsen et al., 2003; Marin et al., 2001; Raho et al., 2008) almost uninformative (Wolny et al., 2020). To overcome this issue Raho et al. (2008, 2013) suggested that the mitochondrial gene of the cytochrome *c* oxidase I (*cox*1) may be more appropriate in distinguishing *D. acuminata* from *D. ovum* and *D. sacculus*.

Numerous field studies (Batifoulier et al., 2013; Berland et al., 1995; Delmas et al., 1993; Gentien et al., 1995; Lassus et al., 1988; Maestrini, 1998) and observations as part of the REPHY monitoring program have led to a better understanding of the biology, toxin-production and ecology of *Dinophysis* spp. on

French coasts. Nonetheless, attempts to culture *Dinophysis* on autotrophic or mixotrophic modes (Maestrini et al., 1995) have failed until elucidation of the three-link food chain (cryptophyte-ciliate-dinoflagellate) and successful establishment of *Dinophysis acuminata* cultures (Park et al., 2006). Following this breakthrough discovery, several *Dinophysis* spp. have been maintained in culture, allowing combined studies of the morphology, genetics, ecophysiology and toxin profiles on the same strains.

The aim of this work was to characterize the genetic and morphological variability as well as the toxin profiles of the dominant species of *Dinophysis* isolated from French coastal waters, including the English Channel, the Bay of Biscay (Atlantic Ocean) and the Mediterranean Sea. A set of 30 monoclonal cultures including strains of the *D. acuminata*-complex (putatively *D. acuminata* and *D. sacculus*), *D. acuta, D. caudata* and *D. tripos* have been isolated from different locations between 2015 and 2019.

2. Material and methods

2.1 Sampling

Plankton net-haul (10 µm mesh) and Niskin bottle samples were collected at twenty different sites in the English Channel, Atlantic and Mediterranean coastal waters and over several seasons from May 2015 to August 2019 (Fig.1, Table 1). *Dinophysis* cells were isolated using a drawn glass micropipette under an inverted IM35 microscope (Carl Zeiss, Oberkochen, Germany), washed three times and transferred to a 4-well cell culture plate (Thermo Scientific ®, Waltham, United States).

2.2 In vitro culturing of **Dinophysis** *spp.*

Thirty monoclonal strains of *Dinophysis* (table 1) were grown in diluted K/2(-Si)/ L1/20 (-Si) culture media (Guillard and Hargraves, 1993) prepared with filtered seawater (0.2 µm Steritop Corning ®, Corning, United States) at pH 8.2 and a salinity of 35. They were maintained in a thermo-regulated room at 17°C and provided ~ 90 µmol m^2 s^{-1} PAR (photosynthetically active radiation) on a 12h light: 12h dark cycle in 250 mL Erlenmeyer flasks. Irradiance was delivered by Osram Fluora 36W (Munich, Germany) and Philips Daylight 36W (Amsterdam, The Netherlands). They were periodically fed on a basis of a 1:1 ratio (predator: prey) with the marine ciliate *Mesodinium rubrum* (MrDK-2009) isolated from Helsingør harbor (Denmark) in 2009. The cryptophyte *Teleaulax amphioxeia* (AND-0710) isolated in

241 2007 from Huelva (Southwest Spain) was added as prey to the
242 ciliate twice a week. The cryptophyte and the ciliate were grown in
243 L1 -Si medium. All cultures were non- axenic.

244 ***2.3 Determination of growth rate***

245 Cell densities were determined on five culture triplicates of
246 *D. acuta*, *D. caudata* and *D. tripos* and two subclades of *D.*
247 *acuminata*-complex, the cells were counted in 10 mL
248 sedimentation chambers under a Zeiss Invertoskop D microscope
249 (Carl Zeiss AG, Oberkochen, Germany), after fixation with acidic
250 Lugol's solution.

251 The average growth rates (μ, day^{-1}) of *Dinophysis* species were
252 calculated over exponential growth as $\mu = \ln (C_2/C_1)/ t_2 - t_1$

253 where C2 and C1 are the concentrations of the cells ($cell \cdot mL^{-1}$) at
254 experimental time 2 and time 1 (day) and μ (day^{-1}) is the growth
255 rate (Guillard, 1973).

256 ***2.4 Microscopy observations***

257 Living cells of the strains studied were observed and
258 measured using a Zeiss Axio Observer D microscope (Carl Zeiss
259 Microscopy, Jena, Germany) equipped with an AxioCam MrC
260 camera. Measurements were taken as the largest dimensions of cell

body (i.e. length and depth in lateral views), excluding cingular and sulcal lists.

For scanning electron microscopy, cells from the cultures were fixed with 2% formaldehyde and then washed several times in deionized water purified at 18 $M\Omega \cdot cm^{-1}$ through a Milli-Q integral 3 system (Merck Millipore, Meyzieu, France). Then, they were filtered on membranes (1.2 µm pores, 19 mm diameter, Merck Millipore, Meyzieu, France), and subsequently processed as described in Chomérat et al. (2019).

2.5 Amplification and sequencing

DNA amplification and sequencing was performed on 24 strains maintained in culture (Table 1). Due to the mixotrophic nature of *Dinophysis* spp. and in order to avoid any contaminations by preys, individual cells were isolated from live cultures by pipetting under an inverted microscope IX51 (Olympus, Tokyo, Japan). Then, they were rinsed in several drops of nuclease-free distilled water, and transferred into a 0.2 mL PCR tube. Nuclear ribosomal genes (ITS–5.8S region and LSU D1–D2) and mitochondrial (mtDNA) cytochrome *c* oxidase I gene (*cox1*) were amplified to allow the characterization from both markers. To increase the number of amplicons, semi-nested-PCR reactions were performed. After the first amplification step, a second

amplification was carried out using 1µL of the PCR product of the first reaction as template, and primers that bind to the target located within the sequence amplified at the first PCR step.

The PCR reaction mixtures (25 µL) contained 1 cell of *Dinophysis*, 12.5 µL of PCR Master Mix (Promega, Foster City, CA, USA), 6.5 µL of DNA free water and 2.5 µL of forward and reverse (10 nM). For the second round of PCR, 1 µL of the amplicon produced in the first step was used as template. Primers used for both rounds of PCR amplifications are given in Table 2. Amplifications were carried out in a thermocycler Tprofessional (Biometra, Göttingen, Germany) with an initial denaturation at 95°C for 10 min, 35 cycles at 95°C for 1 min, 62°C for 1 min and 72°C for 3 min, followed by a 10 min extension step at 72°C.

PCR-amplified products were visualized on an agarose gel after electrophoresis and the positive samples were purified using the ExoSAP-IT PCR Product Cleanup reagent (Affymetrix, Cleveland, OH, USA).The Big Dye Terminator v3.1 Cycle Sequencing Kit (Applied Biosystems, Tokyo, Japan) was used for sequencing the amplicon generated at the second round of PCR. Primers and excess dye-labelled nucleotides were first removed using the Big Dye X-terminator purification kit (Applied

Biosystems, Foster City, CA, USA). Sequencing products were run on an ABI PRISM 3130 Genetic Analyzer (Applied Biosystems).

2.6 Alignment and phylogenetic analyses

Sequences obtained for the 24 strains studied have been used in two distinct datasets (ITS–5.8S region and LSU rDNA, and *cox1*) for phylogenetic reconstructions, i.e. all *D. acuminata* and *D. sacculus* strains and at least one strain each of the three morphologically easily identifiable species (*D. acuta*, *D. caudata* and *D. tripos*). For the ITS–5.8S region and LSU rDNA, sequences of the 24 strains were aligned with 52 sequences of *Dinophysis* spp. retrieved in GenBank and *Phalacroma rapa* as external group, using MUSCLE algorithm in the MEGA X software version 10.1.7 (Kumar et al., 2018). This step was followed by refinement by eye. The resulting matrix included 77 sequences and 1633 aligned positions (including gaps). For the *cox1* dataset, a matrix of 52 sequences and 718 characters was obtained by alignment with Clustal W using the MEGA software.

For each data set, evolutionary models were examined using maximum likelihood (ML) and Bayesian Inference analysis (BI). The evolutionary model was selected using jModelTest version 2.1.10 (Darriba et al., 2012). According to Akaike information criterion (AIC) and Bayesian information criterion

(BIC), a general time reversible (GTR) model with a gamma correction (G) for among-site rate variation and no invariant sites was chosen for the ITS–LSU dataset while a Tamura-Nei model (TN93) with no invariant sites was chosen for the *cox1* dataset.

Maximum likelihood analyses were performed using PhyML version 3.0 (Guindon et al., 2010), and Bayesian analyses were run using Mr Bayes version 3.1.2 (Ronquist and Huelsenbeck, 2003). Parameters used in each analysis are given in supplementary table S1. Bootstrap analysis (1000 pseudoreplicates) was used to assess the relative robustness of branches of the ML tree. Initial Bayesian analyses were run with a GTR model (nst=6) with rates set to gamma for both datasets. Each analysis was performed using four Markov chains (MCMC), with four millions cycles for each chain. Trees were saved every 100 cycles and the first 4000 trees were discarded. Therefore, a majority-rule consensus tree was created from the remaining 36,001 trees in order to examine the posterior probabilities of each clade. Bootstraps values below 65 and posterior probabilities below 0.70 representing absence of support were not shown but indicated as '-'.

346 The consensus trees were edited using Seaview. The best ML
347 phylograms are shown with robustness values for each node
348 (ML/BI).

349 ***2.7 Toxin analysis***

350 ***2.7.1 Reagent and chemicals***

351 Formic acid (FA, 98%) and ammonium formate (10M in
352 solution) were purchased from Sigma Aldrich (Darmstadt,
353 Germany), Acetonitrile (ACN) and methanol (MeOH) was
354 purchased from Honeywell (Seelze, Germany). Water was
355 deionized and purified at 18 $M\Omega \cdot cm^{-1}$ through a Milli-Q integral
356 3 system (Merck Millipore, Meyzieu, France). Certified
357 reference materials (OA, DTX1, DTX2, and PTX2) were
358 purchased from the National Research Council Canada (NRC-
359 CNRC, Halifax, Nova Scotia, Canada) and the non-certified C8-
360 diol ester of OA were purchased from Cifga (via Novakits,
361 Nantes, France).

362 ***2.7.2 Extraction procedures***

363 Samples (10 mL) of *Dinophysis* culture were collected at
364 the end of the exponential growth phase and centrifuged at 3500 *g*,
365 4°C for 15 min. The supernatant was removed and cell pellets were
366 extracted twice with 0.5 mL MeOH using an ultrasonic bath (Elma,

Singen, Germany) at 25 KHz during 15 min in sweep mode. Once cells were disrupted, the supernatants were collected and combined after centrifugation (at 3500 *g*, 4°C, 15 min). The final extracts (0.5 mL) were filtered through a Nanosep MF 0.2 µm filter (Pall, Northborough, MA, USA), and stored at -20°C until LC-MS/MS analysis.

2.7.3 Liquid chromatography coupled to tandem mass spectrometry

LC-MS/MS analysis were performed using a HPLC system (UFLC XR Nexera, Shimadzu, Japan) coupled to a hybrid triple quadrupole/ion-trap mass spectrometer API 4000 QTrap (SCIEX, Redwood City, CA, USA) equipped with a turboV® ESI source.

Chromatographic separation was carried out on a reversed-phase C18 Kinetex column (100 Å, 2.6 µm, 50 × 2.1 mm, Phenomenex, LePecq, France) at 40 °C using a mobile phase composed of water (A) and 95% acetonitrile/water (B) both containing 5 mM ammonium formate and 50 mM formic acid. The flow rate was set to 0.4 mL·min^{-1} and the injection volume was 5 µL. Mass spectrometric detection was performed in either negative or positive ionization mode using Multiple Reaction Monitoring (MRM) scanning. To achieve a better separation and sensitivity for each toxin group, three LC-MS/MS methods were

created (for ESI parameters and the *m/z* transitions see Table 3). The gradients were described as follows:

(i) For OA and DTX analogs, mobile phase was raised from 10% to 50% B in 2 min, to 90% B over the next 4.5 min, then held for 1 min before return to the initial condition (10% B) followed by a re-equilibration period of 3.5 min.

(ii) For PTXs, mobile phase was held for 1 min at 10% B, then raised from 10% to 60% B in 2 min, and to 90% B over the next 4 min, held for 2 min before return to the initial condition (10% B) followed by a re-equilibration period (10% B) of 3.0 min.

(iii) For OA diol esters, separation was achieved using a mobile phase gradient from 10% to 50% B in 2 min, to 95% B over the next 4.5 min, held for 3.5 min before return to the initial condition (10% B) in 1 min and a re-equilibration period (10% B) of 5 min.

The instrument control, data processing and analysis were conducted using Analyst software 1.6.3 (Sciex, Redwood City, CA, USA). Due to the lack of standards, quantification was performed using linear calibration curves generated from reference standards of OA, DTX2, DTX1, PTX2 and C8-diol ester of OA.

411 The limits of detection (LODs) and quantification (LOQs) for
412 available standards were determined with the ordinary least-
413 squares regression method (Sanagi et al., 2009; Vial and Jardy,
414 1999)(Table 3), and also recorded on a cellular basis [pg·cell^{-1}]
415 (Table S2).

416

417 # 3. Results

418 ## *3.1 Taxonomic identification of French strains of* **Dinophysis**
419 ***spp.***

420 ### *3.1.1 Molecular phylogenetic data*

421 The phylogenetic analysis inferred from the LSU rDNA
422 nuclear gene revealed that the sequences obtained for 24 French
423 strains clustered in four different clades. Nineteen sequences
424 clustered into a group of sequences identified as *D. acuminata*-
425 complex, three sequences within *D. acuta,* one sequence within
426 *D. caudata* and one within *D. tripos* (Fig. 2). Interestingly, all 19
427 sequences of the *D. acuminata*-complex were identical, and no
428 difference was found with respect to their geographical origin (Fig.
429 2). Additionally, several sequences of this clade retrieved in
430 GenBank have been ascribed to different names such as
431 '*D. acuminata*', '*D. ovum*' (e.g. MN565962) and '*D. sacculus*'

(e.g. AY040583), but from a molecular point of view, they all appeared almost similar and impossible to distinguish based on sequence data.

The phylogenetic ML and BI trees inferred from *cox1* gene were congruent and the 24 sequences of French strains clustered into four clades (Fig. 3). The sequences of strains IFR-DTR-01Ar and IFR-DCA-04Tr identified as *D. tripos* and *D. caudata*, respectively, were identical and clustered together into a clade comprising *D. miles*, *D. tripos* and *D. caudata*, almost unsupported by the bootstrap values. Sequences of the three strains identified as *D. acuta*, namely IFR-DAC-03Ke, IFR-DAC-02Lc and IFR-DAC-01Ar, grouped together with the sequence HQ681272 identified as *D. acuta*, with a moderate bootstrap support.

The remaining 19 sequences clustered in the *D. acuminata*-complex (Fig. 3). Within this clade, two subgroups of sequences were found: the subclade A included 8 strains from France (3 from English Channel and 5 from Atlantic Ocean), and 14 sequences from various origins (Korea, Greece, USA and Spain) identified as '*D. acuminata*'. The subclade B comprised 11 sequences from French strains (4 from Atlantic Ocean and 7 from Mediterranean Sea) and two sequences from Spain (KC576782 and KY849911) identified as '*D. sacculus*'. However, within the *D. acuminata*-

454 complex, the sequences of these two subclades differed by only
455 one nucleotide (at position 136), with a 'G' in all sequences of
456 subclade A replaced by an 'A' in all sequences of subclade B
457 (Fig. 4). This unique difference resulted in a poor resolution in the
458 phylogenetic analysis and thereby a low bootstrap support of the
459 branch (Fig. 3). Although they have a 'G' at position 136, as for all
460 other sequences of subclade A, two Galician sequences were well
461 divergent from all others of this subclade with 11 and 2 differences
462 for sequences AM931582 and HQ681583, respectively.

463 ***3.1.2 Morphological features and growth of* D. acuta, D. caudata**
464 ***and* D. tripos *strains***

465 Cells of *D. acuta* strains had a typical outline with a wider
466 depth ('width') under the median part, and a triangular shape at
467 their posterior end (Fig. 5A). Cells of the strain IFR-DAC-01Ar
468 were 67.1 ± 2.0 µm long and 46.4 ± 2.7 deep, with a L/D ratio
469 varying from 1.33 to 1.63 (Table 4).

470 Cells of *D. caudata* were easily recognized with their
471 unique and prominent ventral projection of the hypotheca (Fig.
472 5B). Cells from strain IFR-DCA-04Tr were 81.8 ± 2.4 µm long
473 and 43.3 ± 1.9 µm deep, with an L/D ratio varying from 1.75 to
474 2.03 (Table 4).

475 Cells of *D. tripos* were characterized by their large size and
476 the presence of two antapical projections. The dorsal projection
477 ('horn') was shorter than the ventral one which was more
478 prominent (Fig. 5C). Cells of the strain IFR-DTR-01Ar were 97.6
479 ± 3.0 µm long and 48.7 ± 3.3 µm deep, with a L/D ratio varying
480 from 1.78 to 2.37 (Table 4).

481 During the exponential growth phase, the average growth
482 rates (µ) of the strains belonging to these three species ranged from
483 0.20 ± 0.01 day^{-1} for *D. caudata* to 0.22 ± 0.02 day^{-1} and 0.23 ±
484 0.03 day^{-1} for *D. tripos* and *D. acuta*, respectively.

485 ***3.1.3 Morphological features, variations and growth of strains of***
486 ***the* D. acuminata-*complex***

487 Cells that belong to strains of the *D. acuminata*-complex
488 were more or less oval, with a variable shape of the dorsal margin
489 from convex to straight (Figs 6 A-H). Among five strains studied
490 for morphometry, average length ranged from 45.4 to 49.9 µm
491 while average depth ranged from 28.7 to 33.6 µm (Table 4) and
492 size did not appear significantly different among these strains
493 (Mann-Whitney tests, not shown). In addition, the average growth
494 rates of the two strains of the *D. acuminata* complex ranged from
495 0.41 ± 0.02 day^{-1} for the strain IFR-DAU-0.2Ar, clustering in
496 subclade A putatively ascribed to '*D. acuminata*' to 0.43 ± 0.01

497 day^{-1} for the strain IFR-DSA-0.1 Lt clustering in subclade B
498 (‘*D. sacculus’*). Growth rates for these *D. acuminata* strains were
499 thus twice as high as those of the aforementioned strains of
500 *D. caudata*, *D. tripos* and *D. acuta*.
501 In order to further investigate morphological variations of
502 strains within the *D. acuminata*-complex in relation with molecular
503 data, the morphology of strains clustering in subclade A putatively
504 ascribed to ‘*D. acuminata*‘ (IFR-DAU-03An, IFR-DAU-01Es,
505 IFR-DAU-01Ca, IFR-DAU-01Ke and IFR-DAU-02Ar) and
506 subclade B putatively ascribed to ‘*D. sacculus*’ (IFR-DSA-01Lt,
507 IFR-DSA-02Th) in the phylogeny inferred from *cox*1 have been
508 studied by SEM. In strains of subclade A, cells with an oval shape
509 and a typical convex dorsal margin were observed in the strains
510 from the English Channel (IFR-DAU-03An, IFR-DAU-01Es, IFR-
511 DAU-01Ca) (Fig. 6A–C). In strains from the Atlantic Ocean, the
512 shape was more variable and some cells were more rectangular
513 with a straight dorsal margin (Fig. 6D). Within strain IFR-DAU-
514 02Ar (Fig. 6E–H), some specimens with a dorsal margin varying
515 from convex on the posterior side (Fig. 6E–F) to straight (Fig. 6G–
516 H) were observed. Depending on the age of the specimens, the
517 ornamentation was found to be variable, from smooth (Fig. 6H) to
518 conspicuously foveate (Fig. 6G). In the two strains of subclade B

519 analyzed, morphology was very variable among cells. In both
520 strains IFR-DSA-01Lt from Atlantic Ocean (Fig. 7A–D) and IFR-
521 DSA-02Th from the Mediterranean area (Fig 7E–H), a continuum
522 of shapes was observed, including cells with a concave dorsal
523 margin and a reniform shape (Fig. 7A, B, E), cells with a straight
524 dorsal margin and almost rectangular (Fig. 7C, F) and cells with a
525 convex dorsal margin (Fig. 7D, G–H). Hence, within-strain
526 morphological variability was high in these strains.

527 ***3.2 Toxin profiles***

528 In this study, LC-MS/MS analyses of toxin contents and
529 profiles were carried out on all 30 *Dinophysis* strains isolated from
530 different locations of the French coastal waters (English Channel,
531 Atlantic Ocean, and Mediterranean Sea). Toxin profiles appeared
532 remarkably conserved for each morphospecies, irrespective of their
533 geographical origin, and five profiles could be identified (Figs 3,
534 S1). Overall, the most abundant toxin was PTX2, being the major
535 compound in *D. tripos*, *D. caudata* and *D. acuta*. Higher PTX2
536 contents per cell were found in *D. tripos* (176 pg·cell^{-1}) and
537 *D. caudata* (39–200 pg·cell^{-1}) and no OA or DTXs were detected
538 (Table S2). The toxin profile of *D. acuta* was characterized by the
539 presence of DTX2 in all strains (Figs 3, S1), again with PTX2 as
540 the major toxin (>50%) and OA present in moderate to high

amounts (10 - 38 pg·cell^{-1}). The Mediterranean strain, IFR-DAC-01Po, showed a low total toxin content (24 pg·cell^{-1}) by comparison with the other strains (59 - 149 pg·cell^{-1}) from the Atlantic Ocean (Table S2, Fig. S1).

Interestingly, within the *D. acuminata*-complex, two very different toxin profiles were observed (Fig. 3). The eight strains clustering within subclade A in *cox1* phylogeny (i.e. '*D. acuminata*', Fig. 3) contained only OA, with all other compounds below LOD (Table S2). The amount of OA varied greatly among the 8 strains analyzed, and, except for one strain, all others contained 32 to 96 pg·cell^{-1} (Table S2). In contrast, the 11 strains clustering into subclade B ('*D. sacculus'*) showed a more complex profile with PTX2 as the major compound (> 60%) and low proportions of OA (Fig. 3). Additionally, C9-diol ester of OA was detected in seven of the eleven strains analyzed. Except in two strains from the Atlantic Ocean IFR-DSA-01Lo and IFR-DSA-01Me, in which it accounted for about 30% of the toxin content (Figs 3, S1), this compound was present as a minor toxin (<9 %) in the other five strains (Table S2).

4. Discussion

562 ***4.1 Molecular identification of strains***

563 Phylogenetic analyses indicated that molecular data are
564 congruent with morphological features to identify unambiguously
565 four species, i.e. *D. acuta*, *D. caudata*, *D. tripos* and *D. acuminata*-
566 complex. Molecular analyses performed on two genetic markers,
567 ITS−LSU rDNA region and mitochondrial *cox1,* produced a rather
568 similar overall topology, but some clades were differently resolved
569 depending on the region analyzed. The present data suggest that
570 *cox1* fails to discriminate species although morphologically easily
571 recognizable, such as *D. caudata* and *D. tripos,* and which are
572 consistently separated by ITS–5.8S region and LSU rDNA
573 sequences. For this reason, ITS and LSU rDNA regions appear
574 generally as better taxonomic markers than *cox1,* which has
575 already been shown to be poorly informative for the taxonomy of
576 certain dinoflagellates (e.g. Penna et al. 2014).

577 ***Case of the* D. acuminata-*complex***

578 In the present study, sequences of 19 strains from various
579 geographical origins were acquired and the absence of any
580 divergence within ITS and LSU rRNA regions suggests that they
581 likely belong to the same taxon. This finding is congruent with
582 previous studies showing that LSU rDNA nuclear gene and ITS
583 region did not separate sequences from the *D. acuminata*-complex,

584 whereas other species are resolved (Guillou et al., 2002; Stern et
585 al., 2014; Wolny et al., 2020, Zhang et al., 2008,). Nevertheless, a
586 divergence was found among strains, with a consistent one-base
587 mismatch in *cox1* sequence of the two subclades A and B. The use
588 of the mitochondrial gene *cox*1 has been proposed by Raho et al.
589 (2013) who successfully discriminated species of the complex
590 (*D. acuminata*, *D. ovum*, *D. sacculus*) but they based their
591 interpretation on a large divergence of sequence AM931582
592 (ascribed to *D. acuminata*) differing by 17 and 15 mismatches with
593 the Galician sequences AM931583 (*D. ovum*) and KC576782
594 (*D. sacculus*), respectively. However, similar to the study by Park
595 et al. (2019), our data confirm that all *cox1* sequences of
596 *D. acuminata*-complex from various locations worldwide are
597 remarkably similar, while none was closely related to the Galician
598 sequence AM931582, suggesting the possibility of sequencing
599 errors in this sequence. Hence, this sequence should not be
600 considered as a reference for *D. acuminata*, and excluding it, the
601 two subclades identified in our phylogenetic analysis inferred from
602 *cox1* gene diverge by 1 base pair only, which is a small divergence
603 to support a distinction at species level. Since this difference was
604 found in a median part of the sequence, it is likely not artefactual
605 nor influenced by the primers. From a functional point of view,

606 this mutation alters the first position of a codon of the subunit of
607 the cytochrome *c* oxydase I and the 'GTA' found in subclade A is
608 replaced by 'ATA' in the subclade B. This alteration induces a
609 conservative replacement of an amino acid, since valine (subclade
610 A) and isoleucine (subclade B) have similar biochemical properties
611 which does generally not affect the function of proteins.
612 Interestingly, the two groups of strains (subclades A and B)
613 present a clear regional pattern, and subclade A was the unique
614 genotype present in the English Channel, both subclades were
615 present in the Atlantic Ocean, while in the Mediterranean area,
616 only strains of subclade B were found. This situation coincides
617 exactly with previous reports showing that natural samples from
618 the English Channel contained only '*Dinophysis acuminata*', those
619 of the Atlantic Ocean a mix of '*D. acuminata'* and '*D. sacculus'*,
620 or intermediate forms difficult to identify, while no typical
621 '*D. acuminata'* has been found from Mediterranean area (Lassus
622 and Bardouil, 1991; Zingone et al., 1998). Hence, based on these
623 data, strains of subclade A can putatively be interpreted as
624 '*D. acuminata*' while those of subclade B might correspond with
625 '*D. sacculus*' although the distinction at species-level is highly
626 questionable.

627 ***The* D. acuminata / D. sacculus *taxonomic issue***

The difficult interpretation of *D. sacculus* and its complex taxonomy have already been well summarized and discussed by Zingone et al. (1998). They emphasized that the morphological distinction of *D. acuminata* and *D. sacculus* has been problematic not only in early studies (*e.g.*, Pavillard 1905) but also more recently for specimens from the Spanish and French Atlantic coast (Bravo et al., 1995; Lassus and Bardouil, 1991) where both species are present (Zingone et al., 1998). Species identification in the *D. acuminata*-complex has been traditionally based on the outline of cells as a major character, but several authors illustrated the morphological variability of *D. acuminata* in natural populations (Bravo et al., 1995; Lassus and Bardouil, 1991; Zingone et al., 1998). Recently, Park et al. (2019) summarized these variations reported from numerous studies worldwide and established a typology of 4 different forms, ranging from oval to elongate oval and with a more or less symmetric shape, and noticed that depending on the populations, the antapex varied from rounded to tapered. According to Park et al. (2019), cells of type A and B have a rounded antapical end, with cells of type B being longer and more elongated than those of type A. By contrast, cells of type C and D have a more tapered antapical end, with cells of type C being more oval-shaped than those of type D. In that study, the

650 authors concluded that the problematic *D. ovum*, formerly
651 considered as a separate species from *D. acuminata* might be
652 conspecific and corresponds to a particular morphology (type A,
653 Park et al., 2019). Following this typology, natural samples from
654 French coasts (Berland et al., 1995; Lassus and Bardouil, 1991;
655 Nézan, 2000; Truquet et al., 1996; Zingone et al., 1998) belong to
656 three types, namely type B, which is elongated oval with convex
657 sides and a rounded antapex, type C, which is oval with a convex
658 dorsal margin and more or less straight posterior ventral side, and
659 type D, which is elongated oval with a dorsal posterior side
660 inclined and a ventral posterior side straight, resulting in a tapered
661 antapex (Park et al., 2019). Although Zingone et al. (1998) also
662 emphasized the wide range of variations in natural samples,
663 according to these authors, *D. sacculus* may be distinguishable
664 from *D. acuminata* on the basis of the shape of the hypothecal
665 plates which in *D. sacculus* are generally elongated, almost
666 rectangular or sac-like, whereas in *D. acuminata* they are shorter,
667 more convex dorsally and often more slender towards the antapex
668 (Zingone et al., 1998). Following this interpretation, cells of the
669 type B by Park et al. (2019) may correspond well to *D. sacculus*
670 while types C and D better fit with *D. acuminata*. Interestingly,
671 (Nézan, 2000) performed a detailed study of natural populations of

672 *Dinophysis* spp. from French coasts of Brittany (Atlantic Ocean),
673 and she reported the shape of *D. acuminata* to be variable
674 throughout the year, with stocky cells (types C, D) observed at the
675 beginning of spring outbreak, whereas cells then became more
676 elongated (type B) in summer and fall. In contrast with Lassus and
677 Bardouil (1991) who considered the more elongated cells as
678 possible morphotypes of *D. sacculus*, she argued that the slight
679 displacement of the antapex towards the ventral side, giving a
680 slightly oblique apical axis, was a characteristic trait of
681 *D. acuminata,* as suggested by Zingone et al. (1998), and she
682 considered them as summer forms of *D. acuminata* (Nézan, 2000).
683 However, these interpretations of either *D. acuminata* or
684 *D. sacculus* based on wild specimens were impossible to verify in
685 absence of cultured reference material and a
686 molecular/biochemical characterization.
687 The present study represents a new step in the interpretation
688 of '*D. acuminata*' and '*D. sacculus'* by bringing important data
689 from cultured monoclonal strains genetically characterized. In
690 strains of *D. acuminata*-complex clustering in subclade A in *cox1*
691 phylogeny (i.e. '*D. acuminata*'), some specimens were found to
692 have the typical stocky shape illustrated by Nézan (2000), such as
693 in IFR-DAU-03An, IFR-DAU-01Es or IFR-DAU-01Ca isolated

694 from English Channel and they correspond well with the
695 morphology of *D. acuminata*. However, this was not always clear,
696 and cells from strains IFR-DAU-01Ke and IFR-DAU-02Ar,
697 genetically identical, were more elongated, and the slight
698 displacement of the antapex towards the ventral side was
699 sometimes completely absent or rarely observed in some
700 specimens within a given strain. Hence, in the subclade A,
701 considerable morphological variations were found to occur in
702 cultures and following the typology by Park et al. (2019), types A,
703 B and C could be found within a single strain. In the subclade B
704 (ascribed as '*D. sacculus*'), some morphologies were in perfect
705 agreement with the redefinition of *D. sacculus* encompassing *D.*
706 *pavillardii* (as synonym) by Zingone et al. (1998), but large
707 variations also occurred, and within a given strain, it was possible
708 to observe some specimens with a typical concave dorsal margin
709 co-occurring with cells with a straight or convex margin, with a
710 continuum of shapes and which could be attributed to types A and
711 B from Park et al. (2019). According to the traditional
712 interpretation of morpho-species these specimens could be either
713 interpreted as *D. sacculus* f. *reniformis*, *D. sacculus* f. *sacculus* or
714 even *D. acuminata* following the proposal by Zingone et al.
715 (1998). Hence, from the present study, it appears that

morphological variations are important within all strains of the *D. acuminata*-complex, and the shape of the dorsal margin should be used cautiously for taxonomic purposes especially to discriminate the problematic species '*D. acuminata'* and '*D. sacculus'*. Large morphological variations observed in the cultures suggest that the cell shape might change depending on the physiological and nutritional state of cultured cells. It can be hypothesized that the mixotrophic behaviour and kleptoplastidy could modify the overall morphology of cells. Further investigations of morphometric features of different strains at various stages of the feeding process are necessary to confirm this hypothesis in the future. Resolving this issue has important ecological and public health implications and could help to better understand the apparent segregation in space or time of '*D. acuminata*' and '*D. sacculus*', as mentioned by Zingone et al. (1998), or interpret seasonal variations in the morphology of natural populations (Nézan, 2000). Grown under the same experimental conditions the strains of '*D. acuminata' and 'D. sacculus'* isolated from the same geographical area showed very similar growth rate but different to those of the other three species studied, and they were in the range reported in the literature for a Spanish strain of '*D. acuminata'* (García-Portela et

738 al., 2018). However, this result needs to be confirmed on a set of
739 strains which have different geographical origins, and under
740 different environmental conditions of salinity and temperature
741 since *D. sacculus* seems to have a higher affinity for semi-enclosed
742 basins and lagoons in contrast to *D. acuminata* (Zingone et al.,
743 1998).

744 ***4.2 Toxin profiles***

745 *Dinophysis* cultures from French coastal waters showed
746 different and species-conserved toxin profiles for each of the three
747 species *D. acuta*, *D. caudata*, *D. tripos*. However, two different
748 profiles were observed for strains of the *D. acuminata*-complex.
749 Geographical origin of the strains did not seem to have any
750 influence on toxin composition, and for a given genotype (i.e.
751 within each of '*D. acuminata*' and '*D. sacculus'*), the profiles were
752 conserved for strains of various origins. For instance, this is the
753 case for *D. acuta* which is the only species producing DTX2. This
754 finding is consistent with the original identification of DTX2 in
755 shellfish from Ireland in 1992 (Hu et al., 1992a; Pleasance et al.,
756 1990) where *D. acuta* is frequently found (Fux et al., 2009;
757 McMahon et al., 1999). It should be noted that various studies
758 from around Spain, Portugal and Scotland associated the presence
759 of *D. acuta* with DTX2 in both field-sampled cells and cultures of

760 *D. acuta* (Fernández et al., 2006; García-Portela et al., 2018; Swan
761 et al., 2018; Vale and Sampayo, 2000), while DTX2 was not
762 detected in *D. acuta* from New Zealand (MacKenzie et al., 2005).
763 The two species *D. caudata* and *D. tripos* differed from
764 other *Dinophysis* species by exhibiting a profile with PTX2 as the
765 sole toxin detected above LOD. The high amounts of PTX2 found
766 in the present study are in accordance with those reported in
767 cultured strains from Spain and Japan (Basti et al., 2015;
768 Rodríguez et al., 2012). Nevertheless, besides an extraordinary
769 high cellular PTX2 content, a trace amount of DTX1 in *D. tripos*
770 was also observed in a clonal culture from Inokushi Bay (Nagai et
771 al., 2013).

772 The investigation of 19 strains of the *D. acuminata*-
773 complex allowed us to compare the toxin profiles of the two
774 subclades '*D. acuminata*' and '*D. sacculus*' grown under the same
775 experimental conditions. The cultures of '*D. acuminata'*, from
776 either English Channel or Atlantic Ocean always presented a
777 simple toxin profile with only OA detected. While the cultures of
778 '*D. sacculus'* from Atlantic Ocean and Mediterranean Sea showed
779 a more complex profile comprising PTX2 as the major compound
780 and also containing OA and C9-diol OA. Interestingly, the toxin
781 profiles, in terms of type of compounds, of the '*D. sacculus'*

782 strains isolated from the Atlantic Ocean did not differ from those
783 from the Mediterranean lagoons. Although variations in the
784 relative proportion of compounds among the strains of
785 '*D. sacculus'* were detected, the toxin profile always included
786 PTX2 as the major toxin and other components, in contrast to the
787 simple profile observed in '*D. acuminata'* in this study.

788 In addition, several studies conducted in Galicia
789 (northwestern Spain) have shown the same difference in the toxin
790 profile between '*D. sacculus'* and '*D. acuminata'*. The strains of
791 '*D. acuminata'* contained only AO (García-Portela et al., 2018;
792 Hernandez-Urcera et al., 2018), while those of '*D. sacculus'*
793 showed a toxic profile dominated by PTX2 with moderate amounts
794 of AO and traces of DTX1 (Riobó et al., 2013).

795 While toxin composition could appear as a reliable feature
796 separating '*D. acuminata'* from '*D. sacculus'* at least in French
797 and Spanish coastal waters, this specificity of toxin profiles
798 observed within the *D. acuminata*-complex does not seem to be
799 consistent with observations at a broader geographical scale. For
800 instance, strains of '*Dinophysis acuminata'*, DAEP01, DABOF02
801 and DAMV01, isolated from three sites within the northeastern
802 US/Canada coastal region in the Atlantic Ocean are genetically
803 identical with the French strains of '*D. acuminata*' (subclade A,

804 Fig. 4) but they produced PTX2 as the major compound and only
805 low amounts of OA and/or DTX1 (Table 4, Raho et al., 2013;
806 Riobó et al., 2013; Tong et al., 2015), which corresponds to the
807 profile observed in '*D. sacculus*' (subclade B) in the present study.
808 Moreover, PTX2 was reported to be the sole toxin detected in
809 seven cultivated strains of *D. acuminata* from Denmark (Nielsen et
810 al., 2012), but unfortunately no molecular data are available for
811 more comparisons. Furthermore, numerous studies have reported a
812 toxin profile dominated by PTX2 in *D. acuminata* from Norway,
813 which is the type locality of this species, while in New Zealand,
814 Japan, China, Chile, Argentina and North America *D. acuminata*
815 also contained smaller amounts of OA and/or DTX1 (Basti et al.,
816 2018; Fabro et al., 2016; Fux et al., 2011; Gao et al., 2019; Hackett
817 et al., 2009; Hattenrath-Lehmann et al., 2015; Kamiyama and
818 Suzuki, 2009; MacKenzie et al., 2005; Miles et al., 2004b; Suzuki
819 et al., 2009; Tong et al., 2015; Uchida et al., 2018). Similarly, LC-
820 MS analysis of picked cells of *D. acuminata* from northern Chile,
821 solely showed high levels of PTX2 (Blanco et al., 2007). Hence,
822 these data appear conflicting and it is not yet clear whether the
823 toxin profile can potentially be used as a chemotaxonomic
824 indicator related with genetics to separate species/ecotypes or not.

825 The production of C9-diol esters of OA was solely detected
826 in *D. sacculus* in the present study, while *D. acuta* did not produce
827 any such diol-esters above LOD. This finding is in contrast to
828 previous study in our laboratory where a Spanish strain of *D. acuta*
829 produced also a C9-diol ester (Sibat et al., 2018). Diol-esters of
830 OA and DTX1 had originally been identified in cultures of
831 *Prorocentrum lima* (Hu et al., 1992b). It is still a matter of debate
832 whether dinoflagellates produce OA and its analogues DTX1 and -
833 2 *de novo* and store these metabolites as such in the cell or whether
834 more complex derivatives such as diol esters or sulfated diol-esters
835 of OA and its analogues are initially biosynthesized and
836 subsequently transformed during transport inside the cell and
837 during excretion. Thus, further investigations of the toxin
838 production of genetically well-characterized clonal strains from
839 various origins are necessary to clarify that the toxin profile does
840 not change throughout the life-cycle and is not influenced by
841 physiology, growth stage or external factors.

842 The toxin profiles produced by the species or ecotypes also
843 have direct relevance to public health. Various risk assessments of
844 algal metabolites accumulating in shellfish, including latest
845 evidence examined from the New Zealand experience (Boundy et
846 al., 2020), suggest that PTXs pose little or no risk to consumer

847 safety (Lawrence et al., 2011). Nevertheless, *D. sacculus*, even
848 though the main toxin produced is PTX2, also produces OA and
849 esters of OA and must therefore still be considered important in
850 public health-orientated monitoring programs. Furthermore, recent
851 evidence suggests that PTXs may have an impact on oyster
852 recruitment (Gaillard et al., 2020), and therefore all *Dinophysis*
853 species should be re-examined for their production of PTXs and
854 their potential implication in shellfish mortalities.

855

856 5. Conclusion

857 Despite a regular monitoring of *Dinophysis* species in
858 French coastal waters and presence of DSTs in shellfish, it is still
859 difficult to ascertain the contribution of each species to shellfish
860 contamination because of morphological variability and difficult
861 taxonomic identification (Reguera et al. 2012). For the first time in
862 France, the present study based on the analysis of 30 clonal strains
863 from various sites from English Channel, Atlantic Ocean and the
864 Mediterranean area revealed four species identified unambiguously
865 by morphology, molecular data and their toxin content. Although
866 some recurrent species have not yet been successfully isolated such

867 as *D. fortii*, this constitutes the major part of toxic *Dinophysis* spp.
868 found in French coastal waters.

869 For a long time, the identification of the most common and
870 closely related species *D. acuminata* and *D. sacculus* has been
871 highly problematic in natural samples, which has led several
872 authors to consider them as *D. acuminata*-complex (Bravo et al.,
873 1995; Lassus and Bardouil, 1991). Data acquired from 19 strains in
874 the present study fail to clearly separate them as two distinct
875 species, but one base-difference in the *cox*1 gene was consistent to
876 separate '*D. acuminata'* and '*D. sacculus'*, and the toxin content
877 associated was shown to differ among them. Whether they actually
878 represent two separate species or ecotypes (varieties) of a same
879 species cannot be resolved from our data. Molecular data do not
880 support a separation at the species-level, considering that ITS–5.8S
881 and LSU rDNA are generally good taxonomic markers for
882 dinoflagellates. Furthermore, the considerable morphological
883 variability observed in cultured strains seem to indicate that cell
884 morphology shows high plasticity and may change in natural
885 populations due to the environmental conditions, which confirms
886 the observations of variable morphologies in natural samples by
887 Lassus and Bardouil (1991). The existence of two distinct toxin
888 profiles in the strains studied could appear as a reliable feature to

889 separate strains, but conflicting data from the literature and lack of
890 information for well characterized strains prevent the use of this
891 character for taxonomic purpose.

892 The molecular data presented here agree with the previous
893 study by Park et al. (2019) in that *D. sacculus* may be considered
894 to be similar to *D. ovum* and they could represent particular
895 morphotypes of *D. acuminata*. On the other hand, our data from
896 *cox1* gene and toxin profiles suggest a slight divergence of these
897 organisms which is relevant from an ecological point of view:
898 *D. sacculus* has a higher affinity for semi-enclosed basins and
899 lagoons than *D. acuminata* (Zingone et al., 1998). It can be
900 hypothesized that they are not yet genetically divergent enough to
901 be considered as separate species, and they may be ecotypes in an
902 early stage of speciation process (Le Gac et al., 2016). Resolving
903 this species concept issue will not be an easy task, but clonal
904 strains will allow further studies including cross-mating
905 experiments, genetic analyses based on multigene, transcriptomic
906 or even genomic approaches and in-depth analyses of toxin
907 production which will indisputably help to better understand the
908 level of genetic divergence in '*D. acuminata*' and '*D. sacculus*'.

909 Independent of the taxonomic issue, the toxin profiles of
910 the two ecotypes are significantly different in terms of public

911 health impact since PTXs, the major toxins produced by the
912 ecotype '*D. sacculus*', are considered of much lower risk to public
913 health due to their rapid biotransformation in mussels and
914 instability in conditions of the human digestive system.
915 Additionally, the difference in toxin profiles within the
916 "*D. acuminata*" complex but also for other species should prompt
917 us to explore their respective environmental impact and in
918 particular their effect on the recruitment of bivalve molluscs and
919 other marine organisms.

Conflict of interest

The authors declare no conflict of interest.

Authors contributions:

VS and NC designed and supervised the study, drafted the paper and coordinated its revisions. Moreover, VS also coordinated and contributed to establishing and maintaining *Dinophysis* clonal cultures, while NC also performed the microscopic observation and phylogenetic analyses. GB conducted the molecular analysis and sequencing and contributed to drafting and editing the paper. MS and GAR conducted the LC-MS analysis and contributed to drafting and editing the paper. LC performed cells measurements, contributed to establishing and maintaining *Dinophysis* clonal cultures, and to drafting and editing the paper. MPR contributed to the field sampling and editing the paper. VR and FM contributed to establishing and maintaining *Dinophysis* clonal cultures. PH obtained external funding of the study. PH and SG participated in writing and editing the paper.

7 Acknowledgments

940 We thank our colleagues from the Ifremer coastal laboratories for
941 tracking and sampling *Dinophysis* sp: S. Françoise (LER
942 Normandie), A. Doner, A. Duval, A. Terre-Terrillon (LER
943 Bretagne Occidentale), K. Colin, M. Fortune, M. Rétho and A.
944 Schmitt (LER Morbihan Pays de Loire), C.Meteigner (LER
945 Arcachon), E. Abadie and C. Hubert (LER Languedoc Roussillon),
946 F.Marco-Mirales and C.Connes (LER Provence Côte d'Azur). We
947 also thank A. Derrien (LER Bretagne Occidentale) for tracking
948 down DSP toxins monitoring data. We are grateful to Dr. David
949 Jaén (LCCRRPP,Junta de Andalucía, Spain) for generously
950 sharing his cultures of *Teleaulax amphioxeia* (AND-A0710) and
951 Dr. Per Juel Hansen (Marine Biological Section, University of
952 Copenhagen, Helsingør, Denmark) for his strain of *Mesodinium*
953 *rubrum* (MrDK-2009). We also thanks Drs. Satoshi Nagai and
954 Takeshi Kamiyama (National Reasearch Institute of Fisheries and
955 Environment of Inland Sea, Hiroshima, Japan), Dr. Beatriz
956 Reguera and Pilar Rial (Instituto Español de Oceanographia, Vigo,
957 Spain) for their invaluable advices on *Dinophysis* culturing. We
958 extend special thanks to Elisabeth Nézan and Dr. Patrick Lassus
959 who kindly accepted to read and improve the manuscript. This
960 work was funded by the project CoCliME which is part of
961 ERA4CS, an ERA-NET initiated by JPI Climate, and funded by

962 EPA (IE), ANR (FR), BMBF (DE), UEFISCDI (RO), RCN (NO),
963 and FORMAS (SE), with co-funding by the European Union
964 (Grant 690462).

965

966

8 References

Adam, R.D., Ortega, Y.R., Gilman, R.H., Sterling, C.R., 2000. Intervening Transcribed Spacer Region 1 Variability in *Cyclospora cayetanensis*. J. Clin Microbiol. 38, 2339–2343.

Alzieu, C., Lassus, P., Maggi, P., Poggi, R., Ravoux, G., 1983. Contamination des coquillages des côtes bretonnes et normandes par une algue unicellulaire toxique (*Dinophysis acuminata*).Rapp. Tech. No. 4. ISTPM. Nantes, France. Institut Scientifique et Technique des Pêches Maritimes, pp. 33.

Amzil, Z., Sibat, M., Royer, F., Masson, N., Abadie, E., 2007. Report on the first detection of pectenotoxin-2, spirolide-A and their derivatives in French shellfish. Mar. Drugs 5(4), 168-179.

Basti, L., Suzuki, T., Uchida, H., Kamiyama, T., Nagai, S., 2018. Thermal acclimation affects growth and lipophilic toxin production in a strain of cosmopolitan harmful alga *Dinophysis acuminata*. Harmful Algae 73, 119-128. https://doi.org/10.1016/j.hal.2018.02.004

Basti, L., Uchida, H., Matsushima, R., Watanabe, R., Suzuki, T., Yamatogi, T., Nagai, S., 2015. Influence of Temperature on Growth and Production of Pectenotoxin-2 by a Monoclonal Culture of *Dinophysis caudata*. Mar. Drugs 13(12), 7124-7137. https://doi.org/10.3390/md13127061

989 Batifoulier, F., Lazure, P., Velo-Suarez, L., Maurer, D., Bonneton,
990 P., Charria, G., Dupuy, C., Gentien, P., 2013. Distribution of
991 *Dinophysis* species in the Bay of Biscay and possible transport
992 pathways to Arcachon Bay. J. Mar. Syst. 109, S273-S283.
993 Belin, C., Soudant, D., Amzil, Z., 2020. Three decades of data on
994 phytoplankton and phycotoxins on the French coast: Lessons from
995 REPHY and REPHYTOX. Harmful Algae, 101733.
996 https://doi.org/10.1016/j.hal.2019.101733
997 Belin, C., Soudant, D., 2018. Trente années d'observation des
998 microalgues et des toxines d'algues sur le littoral. Editions QUAE,
999 261 pp.
1000 Berland, B.R., Maestrini, S.Y., Grzebyk, D., 1995. Observations
1001 on possible life cycle stages of the dinoflagellate *Dinophysis* cf.
1002 *acuminata*, *Dinophysis acuta* and *Dinophysis pavillardi*. Aquat.
1003 Microb. Biol. 9, 183- 189.
1004 Blanco, J., Alvarez, G., Uribe, E., 2007. Identification of
1005 pectenotoxins in plankton, filter feeders, and isolated cells of a
1006 *Dinophysis acuminata* with an atypical toxin profile, from Chile.
1007 Toxicon 49(5), 710-716.
1008 Boundy, M.J., Harwood, D.T., Kiermeier, A., McLeod, C., 2020.
1009 Pectenotoxins and Okadaic acid group toxins in New Zealand
1010 Bivalve Molluscan Shellfish, 2009-2019: Risk Assessment

1011 Prepared for the Ministry for Primary Industries, Cawthron ed., p.
1012 89.
1013 Bravo, I., Delgado, M., Fraga, S., Honsell, G., Lassus, P.,
1014 Montresor, M., Sampayo, M., 1995. The *Dinophysis* genus:
1015 toxicity and species definition in Europe, In: Lassus, P., Arzul, G.,
1016 Erard, E., Gentien, P., Marcaillou, C. (Eds.), Harmful Marine
1017 Algal Blooms. Lavoisier, Paris, pp. 843-845.
1018 Chomérat, N., Bilien, G., Derrien, A., Henry, K., Ung, A., Viallon,
1019 J., Darius, H.T., Mahana Iti Gatti, C., Roue, M., Herve, F.,
1020 Reveillon, D., Amzil, Z., Chinain, M., 2019. *Ostreopsis*
1021 *lenticularis* Y. Fukuyo (Dinophyceae, Gonyaulacales) from French
1022 Polynesia (South Pacific Ocean): A revisit of its morphology,
1023 molecular phylogeny and toxicity. Harmful Algae 84, 95-111.
1024 https://doi.org/10.1016/j.hal.2019.02.004
1025 Darriba, D., Taboada, G.L., Doallo, R., Posada, D., 2012.
1026 jModelTest 2: more models, new heuristics and parallel
1027 computing. Nat. Methods 9, 772.
1028 Delmas, D., Herbland, A., Maestrini, S.Y., 1993. Do *Dinophysis*
1029 spp. come from the "open sea" along the French Atlantic coast? In:
1030 Smayda, T.J., Shimizu, Y. (Eds.), Toxic Phytoplankton Blooms in
1031 the Sea. Elsevier, New York, pp. 489-494.

1032 Edvardsen, B., Shalchian-Tabrizi, K., Jakobsen, K.S., Medlin,
1033 L.K., Dahl, E., Brubak, S., Paasche, E., 2003. Genetic variability
1034 and molecular phylogeny of *Dinophysis* species (Dinophyceae)
1035 from Norwegian waters inferred from single cell analyses of
1036 rDNA. J. Phycol. 39(2), 395-408.
1037 Fabro, E., Almandoz, G.O., Ferrario, M., Tillmann, U., Cembella,
1038 A., Krock, B., 2016. Distribution of *Dinophysis* species and their
1039 association with lipophilic phycotoxins in plankton from the
1040 Argentine Sea. Harmful Algae 59, 31-41.
1041 https://doi.org/10.1016/j.hal.2016.09.001
1042 Fernández, M.L., Reguera, B., González-Gil, S., Míguez, A., 2006.
1043 Pectenotoxin-2 in single-cell isolates of *Dinophysis caudata* and
1044 *Dinophysis acuta* from the Galician Rías (NW Spain). Toxicon
1045 48(5), 477-490. https://doi.org/10.1016/j.toxicon.2006.05.016
1046 Fux, E., Biré, R., Hess, P., 2009. Comparative accumulation and
1047 composition of lipophilic marine biotoxins in passive samplers and
1048 in mussels (*M. edulis*) on the West Coast of Ireland. Harmful
1049 Algae 8(3), 523-537.
1050 Fux, E., Smith, J.L., Tong, M.M., Guzman, L., Anderson, D.M.,
1051 2011. Toxin profiles of five geographical isolates of *Dinophysis*
1052 spp. from North and South America. Toxicon 57(2), 275-287.

1053 Gaillard, S., Le Goïc, N., Malo, F., Boulais, M., Fabioux, C.,
1054 Zaccagnini, L., Carpentier, L., Sibat, M., Réveillon, D., Séchet, V.,
1055 Hess, P., Hégaret, H., 2020. Cultures of *Dinophysis sacculus*,
1056 *D. acuminata* and pectenotoxin 2 affect gametes and fertilization
1057 success of the Pacific oyster, *Crassostrea gigas*. Environ. Pollut.
1058 265, 114840. https://doi.org/10.1016/j.envpol.2020.114840
1059 Gao, H., Tong, M., An, X., Smith, J.L., 2019. Prey Lysate
1060 Enhances Growth and Toxin Production in an Isolate of
1061 *Dinophysis acuminata*. Toxins 11(1).
1062 García-Portela, M., Reguera, B., Sibat, M., Altenburger, A.,
1063 Rodríguez, F., Hess, P., 2018. Metabolomic profiles of *Dinophysis*
1064 *acuminata* and *Dinophysis acuta* using non-targeted high-
1065 resolution mass spectrometry: effect of nutritional status and prey.
1066 Mar. Drugs 16(5), 143. https://doi.org/10.3390/md16050143
1067 Gentien, P., Lunven, M., Lehaitre, M., Duvent, J.L., 1995. *In situ*
1068 depth profiling of particle sizes. Deep-Sea Res. 42(8), 1297-1312.
1069 Guillard, R.L., 1973. Division rates. In: Stein, J. (Ed.), Handbook
1070 of Phycological Methods. Cambridge University Press, London,
1071 pp. 289-312.
1072 Guillard, R.R.L., Hargraves, P.E., 1993. *Stichochrysis immobilis* is
1073 a diatom, not a chrysophyte. Phycologia 32(3), 234-236.

1074 Guillou, L., Nézan, E., Cueff, V., Erard-Le Denn, E., Cambon-
1075 Bonavita, M.-A., Gentien, P., Barbier, G., 2002. Genetic Diversity
1076 and Molecular Detection of Three Toxic Dinoflagellate Genera
1077 (*Alexandrium*, *Dinophysis*, and *Karenia*) from French Coasts.
1078 Protist 153(3), 223.
1079 Guindon, S., Dufayard, J.F., Lefort, V., Anisimova, M., Hordijk,
1080 W., Gascuel, O., 2010. New algorithms and methods to estimate
1081 maximum-likelihood phylogenies: assessing the performance of
1082 PhyML 3.0. Syst Biol 59.
1083 Guiry, M.D., 2020. In Guiry, M.D. & Guiry, G.M. 2020.
1084 AlgaeBase. World-wide electronic publication, National
1085 University of Ireland, Galway. http://www.algaebase.org; searched
1086 on 28 February 2020.
1087 Hackett, J.D., Tong, M., Kulis, D.M., Fux, E., Hess, P., Biré, R.,
1088 Anderson, D.M., 2009. DSP toxin production de novo in cultures
1089 of *Dinophysis acuminata* (Dinophyceae) from North America.
1090 Harmful Algae 8(6), 873-879.
1091 Hallegraeff, G.M., Lucas, I.A.N., 1988. The marine dinoflagellate
1092 genus *Dinophysis* (Dinophyceae): Photosynthetic, neritic and non-
1093 photosynthetic, oceanic species. Phycologia 27, 25-42.
1094 Hattenrath-Lehmann, T.K., Marcoval, M.A., Mittlesdorf, H.,
1095 Goleski, J.A., Wang, Z., Haynes, B., Morton, S.L., Gobler, C.J.,

2015. Nitrogenous Nutrients Promote the Growth and Toxicity of *Dinophysis acuminata* during Estuarine Bloom Events. PLoS One 10(4), e0124148. https://doi.org/10.1371/journal.pone.0124148

Hernandez-Urcera, J., Rial, P., Garcia-Portela, M., Loures, P., Kilcoyne, J., Rodríguez, F., Fernandez-Villamarin, A., Reguera, B., 2018. Notes on the Cultivation of Two Mixotrophic *Dinophysis* Species and Their Ciliate Prey *Mesodinium rubrum*. Toxins 10(12), p.505. https://doi.org/10.3390/toxins10120505

Hu, T., Doyle, J., Jackson, D., Marr, J., Nixon, E., Pleasance, S., Quilliam, M.A., Walter, J.A., Wright, J.L.C., 1992a. Isolation of a new diarrhetic shellfish poison from Irish mussels. J. Chem. Soc. Ser. (1), 39-41.

Hu, T., Marr, J., DeFreitas, A.S.W., Quilliam, M.A., Walter, J.A., Wright, J.L.C., Pleasance, S., 1992b. New diol esters isolated from cultures of the dinoflagellates *Prorocentrum lima* and *Prorocentrum concavum*. J. Nat. Prod. 55(11), 1631-1637.

Kamiyama, T., Suzuki, T., 2009. Production of dinophysistoxin-1 and pectenotoxin-2 by a culture of *Dinophysis acuminata* (Dinophyceae). Harmful Algae 8(2), 312-317.

Kumagai, M., Yanagi, T., Murata, M., Yasumoto, T., Kat, M., Lassus, P., Rodríguez-Vazquez, J.A., 1986. Okadaic acid as the

1117 causative toxin of diarrhetic shellfish poisoning in Europe. Agric.
1118 Biol. Chem. 50, 2853-2857.
1119 Kumar, S., Stecher, G., Li, M., Knyaz, C., Tamura, K., 2018.
1120 MEGA X: Molecular Evolutionary Genetics Analysis across
1121 Computing Platforms. Mol. Biol. Evol. 35, 1547-1549.
1122 https://doi.org/10.1093/molbev/msy096
1123 Lassus, P., Bardouil, M., 1991. Le complexe *Dinophysis*
1124 *acuminata*: identification des espèces le long des côtes françaises.
1125 Cryptogam. Algol. 12(1), 1-9.
1126 Lassus, P., Bardouil, M., Berthom, J.-P., Maggi, P., Truquet, P., Le
1127 Dean, L., 1988. Seasonal occurrence of *Dinophysis* sp. along the
1128 French coast between 1983 and 1987. Aquat. Living Resour. 1,
1129 155-164.
1130 Lassus, P., Bardouil, M., Truquet, I., Truquet, P., le Baut, C.,
1131 Pierri, M.J., 1985. *Dinophysis acuminata* distribution and toxicity
1132 along the southern Brittany coast (France): Correlation with
1133 hydrological parameters, In: Anderson, D.M., White, A.W., Baden,
1134 D.G. (Eds.), Toxic Dinoflagellates. Elsevier, New York, pp. 159-
1135 164.
1136 Lawrence, J., Loreal, H., Toyofuku, H., Hess, P., Iddya, K.,
1137 Ababouch, L., 2011. Assessment and management of biotoxin

1138 risks in bivalve molluscs. FAO Fisheries and Aquaculture
1139 Technical Paper No. 551, p. 337.
1140 Le Gac, M., Metegnier, G., Chomérat, N., Malestroit, P., Quere, J.,
1141 Bouchez, O., Siano, R., Destombe, C., Guillou, L., Chapelle, A.,
1142 2016. Evolutionary processes and cellular functions underlying
1143 divergence in *Alexandrium minutum*. Mol. Ecol. 25(20), 5129-
1144 5143. https://doi.org/10.17882/45445
1145 Lin, S.J., Zhang, H.A., Spencer, D.F., Norman, J.E., Gray, M.W.,
1146 2002. Widespread and extensive editing of mitochondrial mRNAS
1147 in dinoflagellates. J. Mol. Biol. 320(4), 727-739.
1148 https://doi.org/10.1016/s0022-2836(02)00468-0
1149 MacKenzie, L., Beuzenberg, V., Holland, P., McNabb, P., Suzuki,
1150 T., Selwood, A., 2005. Pectenotoxin and okadaic acid-based toxin
1151 profiles in *Dinophysis acuta* and *Dinophysis acuminata* from New
1152 Zealand. Harmful Algae 4(1), 75-85.
1153 Maestrini, S.Y., 1998. Bloom dynamics and ecophysiology of
1154 *Dinophysis* spp. NATO ASI Series G 41, 242 - 265.
1155 Maestrini, S.Y., Berland, B.R., Grzebyk, D., Spano, A.M., 1995.
1156 *Dinophysis* spp. cells concentrated from nature for experimental
1157 purposes, using size fractionation and reverse migration. Aquat.
1158 Microb. Ecol. 9(2), 177-182.

1159 Marcaillou-Le Baut, C., Masselin, P., 1989. Recent Data on
1160 Diarrhetic Shellfish Poisoning in France, Toxic Marine
1161 Phytoplankton. Granéli E, Sundström B, Edler L, Anderson DM
1162 (eds.) Elsevier, New-York, pp. 487-492.
1163 Marin, I., Aguilera, A., Reguera, B., Abad, J.P., 2001. Preparation
1164 of DNA suitable for PCR amplification from fresh or fixed single
1165 dinoflagellate cells. Biotechniques 30(1), 88-+.
1166 McMahon, T., Silke, J., Cahill, B., 1999. Irish coastal
1167 dinoflagellate blooms and shellfish toxicity. J. Shellfish Res. 18(2),
1168 722-723.
1169 Miles, C.O., Wilkins, A.L., Munday, R., Dines, M.H., Hawkes,
1170 A.D., Briggs, L.R., Sandvik, M., Jensen, D.J., Cooney, J.M.,
1171 Holland, P.T., Quilliam, M.A., Lincoln MacKenzie, A.,
1172 Beuzenberg, V., Towers, N.R., 2004a. Isolation of pectenotoxin-2
1173 from *Dinophysis acuta* and its conversion to pectenotoxin-2 seco
1174 acid, and preliminary assessment of their acute toxicities. Toxicon
1175 43(1), 1-9.
1176 Miles, C.O., Wilkins, A.L., Samdal, I.A., Sandvik, M., Petersen,
1177 D., Quilliam, M.A., Naustvoll, L.J., Rundberget, T., Torgersen, T.,
1178 Hovgaard, P., Jensen, D.J., Cooney, J.M., 2004b. A novel
1179 pectenotoxin, PTX-12, in *Dinophysis* spp. and shellfish from
1180 Norway. Chem. Res. Toxicol. 17(11), 1423-1433.

1181 Nagai, S., Suzuki, T., Kamiyama, T., 2013. Successful cultivation
1182 of the toxic dinoflagellate *Dinophysis tripos* (Dinophyceae).
1183 Plankton and Benthos Research 8(4), 171-177.
1184 Nézan, E., 2000. Episodes à *Dinophysis* dans le Finistère et
1185 variations morphologiques des espèces responsables. R.S.T -
1186 DEL/00-01/Concarneau, p. 31.
1187 https://archimer.ifremer.fr/doc/00037/14847/
1188 Nielsen, L.T., Krock, B., Hansen, P.J., 2012. Effects of light and
1189 food availability on toxin production, growth and photosynthesis in
1190 *Dinophysis acuminata*. Mar. Ecol. Progr. Ser 471, 37-50.
1191 Nunn, G.B., Theisen, B.F., Christensen, B., Arctander, P., 1996.
1192 Simplicity-correlated size growth of the nuclear 28S ribosomal
1193 RNA D3 expansion segment in the crustacean order Isopoda. J.
1194 Mol. Evol. 42, 211-223.
1195 Park, J.H., Kim, M., Jeong, H.J., Park, M.G., 2019. Revisiting the
1196 taxonomy of the "*Dinophysis acuminata* complex" (Dinophyta)'.
1197 Harmful Algae 88, 101657.
1198 https://doi.org/10.1016/j.hal.2019.101657
1199 Park, M.G., Kim, S., Kim, H.S., Myung, G., Kang, Y.G., Yih, W.,
1200 2006. First successful culture of the marine dinoflagellate
1201 *Dinophysis acuminata*. Aquat. Microb. Ecol. 45(2), 101-106.

1202 Pavillard, J., 1905. Recherches sur la Flore Pélagique
1203 (Phytoplancton) de l'Etang de Thau. Montpellier, p.116.
1204 Penna, A., Battocchi, C., Capellacci, S., Fraga, S., Aligizaki, K.,
1205 Lemée, R., Vernesi, C., 2014. Mitochondrial, but not rDNA, genes
1206 fail to discriminate dinoflagellate species in the genus *Ostreopsis*.
1207 Harmful Algae 40, 40-50.
1208 Penna, A., Magnani, M., 1999. Identification of *Alexandrium*
1209 (Dinophyceae) species using PCR and rDNA-targeted probes. J.
1210 Phycol. 35(3), 615-621.
1211 Pleasance, S., Quilliam, M.A., de Freitas, A.S.W., Marr, J.C.,
1212 Cembella, A.D., 1990. Ion-spray mass spectrometry of marine
1213 toxins. II. Analysis of diarrhetic shellfish toxins in plankton by
1214 liquid chromatography/mass spectrometry. Rapid Commun. Mass
1215 Spectrom. 4, 206-213.
1216 Raho, N., Pizarro, G., Escalera, L., Reguera, B., Marín, I., 2008.
1217 Morphology, toxin composition and molecular analysis of
1218 *Dinophysis ovum* Schütt, a dinoflagellate of the "*Dinophysis*
1219 *acuminata complex*". Harmful Algae 7(6), 839-848.
1220 https://doi.org/10.1016/j.hal.2008.04.006
1221 Raho, N., Rodríguez, F., Reguera, B., Marín, I., 2013. Are the
1222 mitochondrial cox1 and cob genes suitable markers for species of
1223 *Dinophysis* Ehrenberg? Harmful Algae 28(0), 64-70.

1224 Reguera, B., Riobó, P., Rodríguez, F., Díaz, P.A., Pizarro, G., Paz,
1225 B., Franco, J.M., Blanco, J., 2014. *Dinophysis* Toxins: Causative
1226 Organisms, Distribution and Fate in Shellfish. Mar. Drugs 12(1),
1227 394-461.
1228 Reguera, B., Velo-Suárez, L., Raine, R., Park, M.G., 2012.
1229 Harmful *Dinophysis* species: A review. Harmful Algae 14, 87-106.
1230 https://doi.org/10.1016/j.hal.2011.10.016
1231 Riobó, P., Reguera, B., Franco, J.M., Rodríguez, F., 2013. First
1232 report of the toxin profile of *Dinophysis sacculus* Stein from LC–
1233 MS analysis of laboratory cultures. Toxicon 76(0), 221-224.
1234 Rodríguez, F., Escalera, L., Reguera, B., Rial, P., Riobo, P., da
1235 Silva, T.D., 2012. Morphological variability, toxinology and
1236 genetics of the dinoflagellate *Dinophysis tripos* (Dinophysiaceae,
1237 Dinophysiales). Harmful Algae 13, 26-33.
1238 Ronquist, F., Huelsenbeck, J.P., 2003. MrBayes 3: Bayesian
1239 phylogenetic inference under mixed models. Bioinformatics. 19,
1240 1572-1574.
1241 Sanagi, M.M., Ling, S.L., Nasir, Z., Hermawan, D., Ibrahim,
1242 W.A., Abu Naim, A., 2009. Comparison of signal-to-noise, blank
1243 determination, and linear regression methods for the estimation of
1244 detection and quantification limits for volatile organic compounds
1245 by gas chromatography. J. AOAC Int. 92(6), 1833-1838.

1246 Scholin, C.A., Anderson, D.M., 1996. LSU rDNA-based RFLP
1247 assays for discriminating species and strains of *Alexandrium*
1248 (Dinophyceae). J. Phycol. 32(6), 1022-1035.
1249 Scholin, C.A., Herzog, M., Sogin, M., Anderson, D.M., 1994.
1250 Identification of group- and strain-specific genetic markers for
1251 globally distributed *Alexandrium* (Dinophyceae). 2. Sequence
1252 analysis of a fragment of the LSU rRNA gene. J. Phycol. 30(6),
1253 999-1011.
1254 Sibat, M., Garcia-Portela, M., Hess, P., 2018. First identification of
1255 a C9-diol-ester of okadaic acid in *Dinophysis acuta* from Galician
1256 Rias Baixas (NW Spain). Toxicon 153, 19-22.
1257 https://doi.org/10.1016/j.toxicon.2018.08.005
1258 Stern, R.F., Amorim, A.L., Bresnan, E., 2014. Diversity and
1259 plastid types in *Dinophysis acuminata* complex (Dinophyceae) in
1260 Scottish waters. Harmful Algae 39, 223-231.
1261 Suzuki, T., Miyazono, A., Baba, K., Sugawara, R., Kamiyama, T.,
1262 2009. LC-MS/MS analysis of okadaic acid analogues and other
1263 lipophilic toxins in single-cell isolates of several *Dinophysis*
1264 species collected in Hokkaido, Japan. Harmful Algae 8(2), 233-
1265 238.
1266 Swan, S.C., Turner, A.D., Bresnan, E., Whyte, C., Paterson, R.F.,
1267 McNeill, S., Mitchell, E., Davidson, K., 2018. *Dinophysis acuta* in

Scottish Coastal Waters and Its Influence on Diarrhetic Shellfish Toxin Profiles. Toxins 10(10).

Tong, M., Smith, J.L., Richlen, M., Steidinger, K.A., Kulis, D.M., Fux, E., Anderson, D.M., 2015. Characterization and comparison of toxin-producing isolates of *Dinophysis acuminata* from New England and Canada. J Phycol 51(1), 66-81.

Truquet, P., Lassus, P., Honsell, G., LeDean, L., 1996. Application of a digital pattern recognition system to *Dinophysis acuminata* and *D-sacculus* complexes. Aquat. Living Resour. 9(3), 273-279.

Uchida, H., Watanabe, R., Matsushima, R., Oikawa, H., Nagai, S., Kamiyama, T., Baba, K., Miyazono, A., Kosaka, Y., Kaga, S., Matsuyama, Y., Suzuki, T., 2018. Toxin Profiles of Okadaic Acid Analogues and Other Lipophilic Toxins in *Dinophysis* from Japanese Coastal Waters. Toxins 10(11), p.457. https://doi.org/10.3390/toxins10110457

Vale, P., Sampayo, M.A.D., 2000. Dinophysistoxin-2: a rare diarrhoeic toxin associated with *Dinophysis acuta*. Toxicon 38(11), 1599-1606.

Vial, J., Jardy, A., 1999. Experimental comparison of the different approaches to estimate LOD and LOQ of an HPLC method. Anal. Chem. 71(14), 2672-2677.

1289 Wolny, J.L., Egerton, T.A., Handy, S.M., Stutts, W.L., Smith, J.L.,
1290 Whereat, E.B., Bachvaroff, T.R., Henrichs, D.W., Campbell, L.,
1291 Deeds, J.R., 2020. Characterization of *Dinophysis* spp.
1292 (Dinophyceae, Dinophysiales) from the mid-Atlantic region of the
1293 United States (1). J. Phycol. 56 (2), 404-424.
1294 https://doi.org/10.1111/jpy.12966
1295 Yasumoto, T., Murata, M., Oshima, Y., Sano, M., 1985. Diarrhetic
1296 Shellfish Toxins. Tetrahedron 41(6), 1019-1025.
1297 Yasumoto, T., Oshima, Y., Sugawara, W., Fukuyo, Y., Oguri, H.,
1298 Igarashi, T., Fujita, N., 1980. Identification of *Dinophysis fortii* as
1299 the causative organism of diarrhetic shellfish poisoning.
1300 Bull.Japan.Soc. Sci. Fish. 46(11), 1405-1411.
1301 Zhang, H., Bhattacharya, D., Maranda, L., Lin, S.J., 2008.
1302 Mitochondrial *cob* and *cox1* genes and editing of the
1303 corresponding mRNAs in *Dinophysis acuminata* from
1304 Narragansett Bay, with special reference to the phylogenetic
1305 position of the genus *Dinophysis*. Appl. Environ. Microbiol. 74(5),
1306 1546-1554.
1307 Zingone, A., Larsen, A., 2020. Zingone, A.; Larsen, J. (Eds)
1308 (2020). Dinophysiales, in IOC-UNESCO Taxonomic Reference
1309 List of Harmful Micro Algae. Available online at
1310 http://www.marinespecies.org/hab. Accessed on 2020-02-28.

1311 Zingone, A., Montresor, M., Marino, D., 1998. Morphological
1312 variability of the potentially toxic dinoflagellate *Dinophysis*
1313 *sacculus* (Dinophyceae) and its taxonomic relationships with *D.*
1314 *pavillardii* and *D. acuminata*. Eur. J. Phycol. 33(3), 259-273.

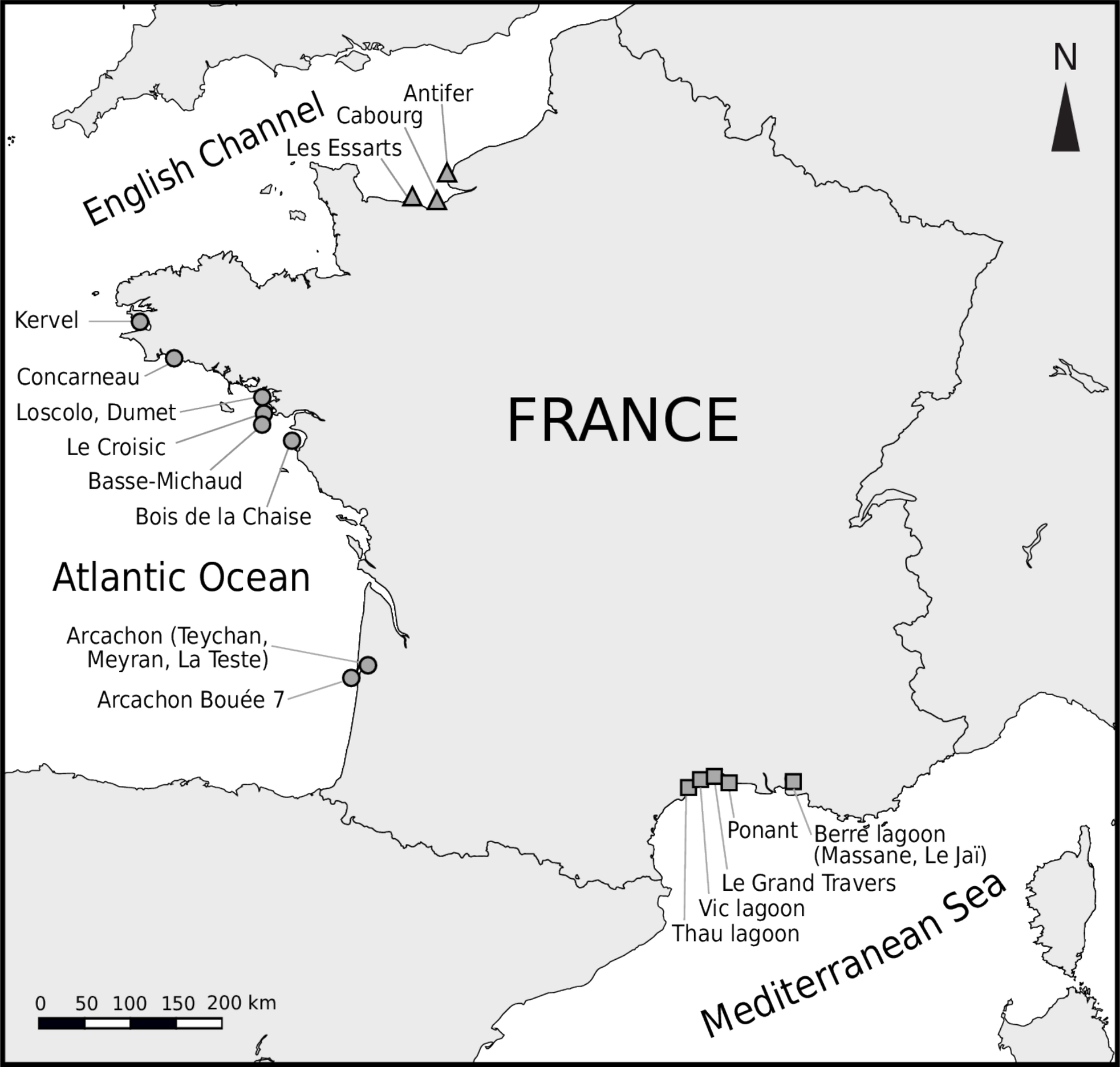
N
English Channel
Antifer
Cabourg
Les Essarts
FRANCE
Kervel
Concarneau
Loscolo, Dumet
Le Croisic
Basse-Michaud
Bois de la Chaise
Atlantic Ocean
Arcachon (Teychan,
Meyran, La Teste)
Arcachon Bouée 7
Ponant
Berre lagoon
(Massane, Le Jaï)
Le Grand Travers
Vic lagoon
Thau lagoon
Mediterranean Sea
0 50 100 150 200 km

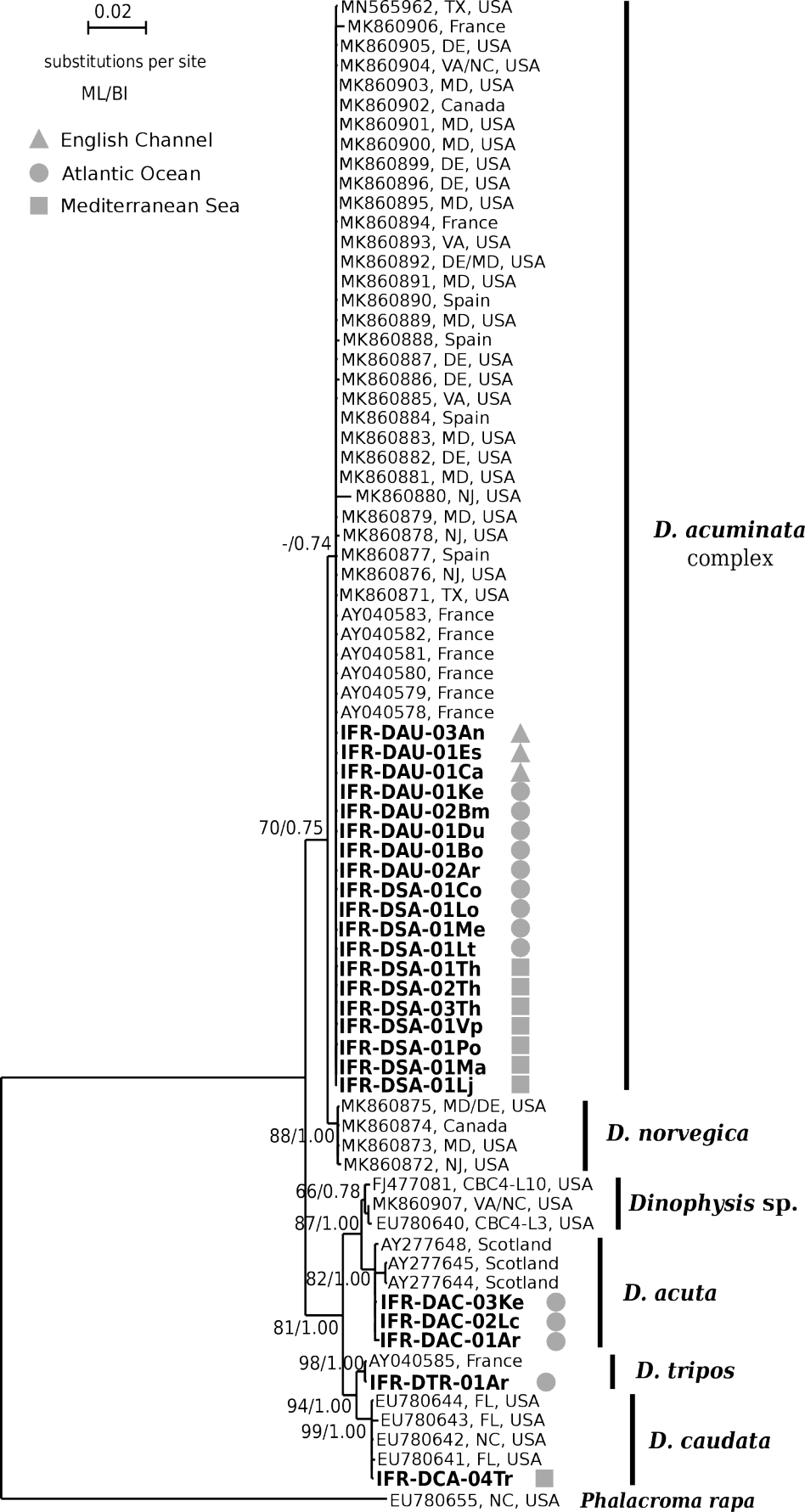
0.02
substitutions per site
ML/BI
English Channel
Atlantic Ocean
Mediterranean Sea
MN565962, TX, USA
MK860906, France
MK860905, DE, USA
MK860904, VA/NC, USA
MK860903, MD, USA
MK860902, Canada
MK860901, MD, USA
MK860900, MD, USA
MK860899, DE, USA
MK860896, DE, USA
MK860895, MD, USA
MK860894, France
MK860893, VA, USA
MK860892, DE/MD, USA
MK860891, MD, USA
MK860890, Spain
MK860889, MD, USA
MK860888, Spain
MK860887, DE, USA
MK860886, DE, USA
MK860885, VA, USA
MK860884, Spain
MK860883, MD, USA
MK860882, DE, USA
MK860881, MD, USA
MK860880, NJ, USA
MK860879, MD, USA
-/0.74
MK860878, NJ, USA
MK860877, Spain
MK860876, NJ, USA
MK860871, TX, USA
AY040583, France
AY040582, France
AY040581, France
AY040580, France
AY040579, France
AY040578, France
IFR-DAU-03An
IFR-DAU-01Es
IFR-DAU-01Ca
IFR-DAU-01Ke
IFR-DAU-02Bm
70/0.75
IFR-DAU-01Du
IFR-DAU-01Bo
IFR-DAU-02Ar
IFR-DSA-01Co
IFR-DSA-01Lo
IFR-DSA-01Me
IFR-DSA-01Lt
IFR-DSA-01Th
IFR-DSA-02Th
IFR-DSA-03Th
IFR-DSA-01Vp
IFR-DSA-01Po
IFR-DSA-01Ma
IFR-DSA-01Lj
D. acuminata complex
MK860875, MD/DE, USA
88/1.00
MK860874, Canada
MK860873, MD, USA
MK860872, NJ, USA
D. norvegica
66/0.78
FJ477081, CBC4-L10, USA
MK860907, VA/NC, USA
87/1.00
EU780640, CBC4-L3, USA
Dinophysis sp.
AY277648, Scotland
AY277645, Scotland
82/1.00
AY277644, Scotland
IFR-DAC-03Ke
IFR-DAC-02Lc
81/1.00
IFR-DAC-01Ar
D. acuta
98/1.00
AY040585, France
IFR-DTR-01Ar
D. tripos
94/1.00
EU780644, FL, USA
99/1.00
EU780643, FL, USA
EU780642, NC, USA
EU780641, FL, USA
IFR-DCA-04Tr
D. caudata
EU780655, NC, USA
Phalacroma rapa

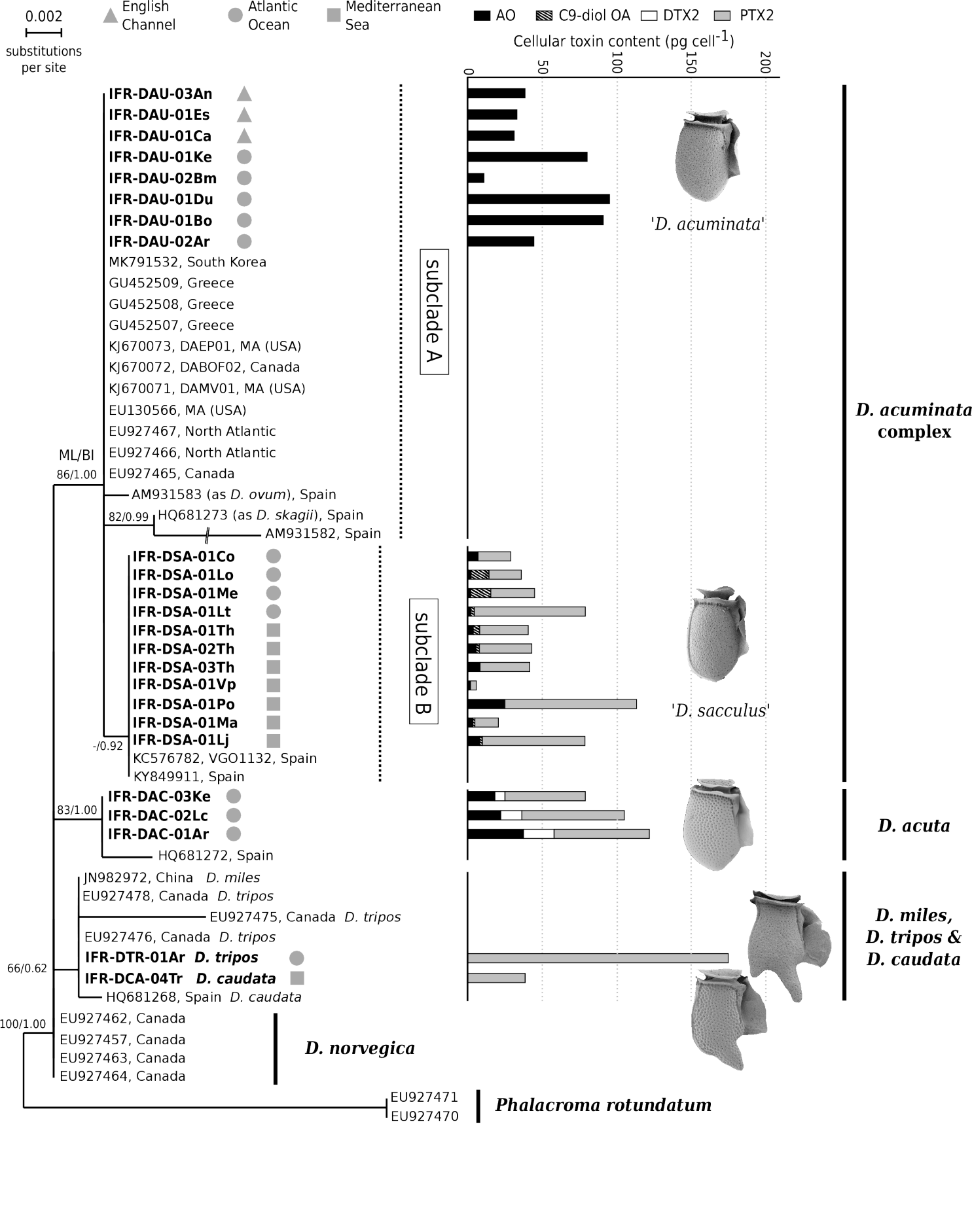
0.002
substitutions per site
English Channel
Atlantic Ocean
Mediterranean Sea
AO
C9-diol OA
DTX2
PTX2
Cellular toxin content (pg cell-1)
0
50
100
150
200
IFR-DAU-03An
IFR-DAU-01Es
IFR-DAU-01Ca
IFR-DAU-01Ke
IFR-DAU-02Bm
IFR-DAU-01Du
IFR-DAU-01Bo
IFR-DAU-02Ar
MK791532, South Korea
GU452509, Greece
GU452508, Greece
GU452507, Greece
KJ670073, DAEP01, MA (USA)
KJ670072, DABOF02, Canada
KJ670071, DAMV01, MA (USA)
EU130566, MA (USA)
EU927467, North Atlantic
EU927466, North Atlantic
EU927465, Canada
ML/BI
86/1.00
AM931583 (as D. ovum), Spain
82/0.99
HQ681273 (as D. skagii), Spain
AM931582, Spain
subclade A
'D. acuminata'
IFR-DSA-01Co
IFR-DSA-01Lo
IFR-DSA-01Me
IFR-DSA-01Lt
IFR-DSA-01Th
IFR-DSA-02Th
IFR-DSA-03Th
IFR-DSA-01Vp
IFR-DSA-01Po
IFR-DSA-01Ma
IFR-DSA-01Lj
-/0.92
KC576782, VGO1132, Spain
KY849911, Spain
subclade B
'D. sacculus'
D. acuminata complex
IFR-DAC-03Ke
IFR-DAC-02Lc
IFR-DAC-01Ar
83/1.00
HQ681272, Spain
D. acuta
JN982972, China D. miles
EU927478, Canada D. tripos
EU927475, Canada D. tripos
EU927476, Canada D. tripos
IFR-DTR-01Ar D. tripos
IFR-DCA-04Tr D. caudata
66/0.62
HQ681268, Spain D. caudata
D. miles, D. tripos & D. caudata
100/1.00
EU927462, Canada
EU927457, Canada
EU927463, Canada
EU927464, Canada
D. norvegica
EU927471
EU927470
Phalacroma rotundatum

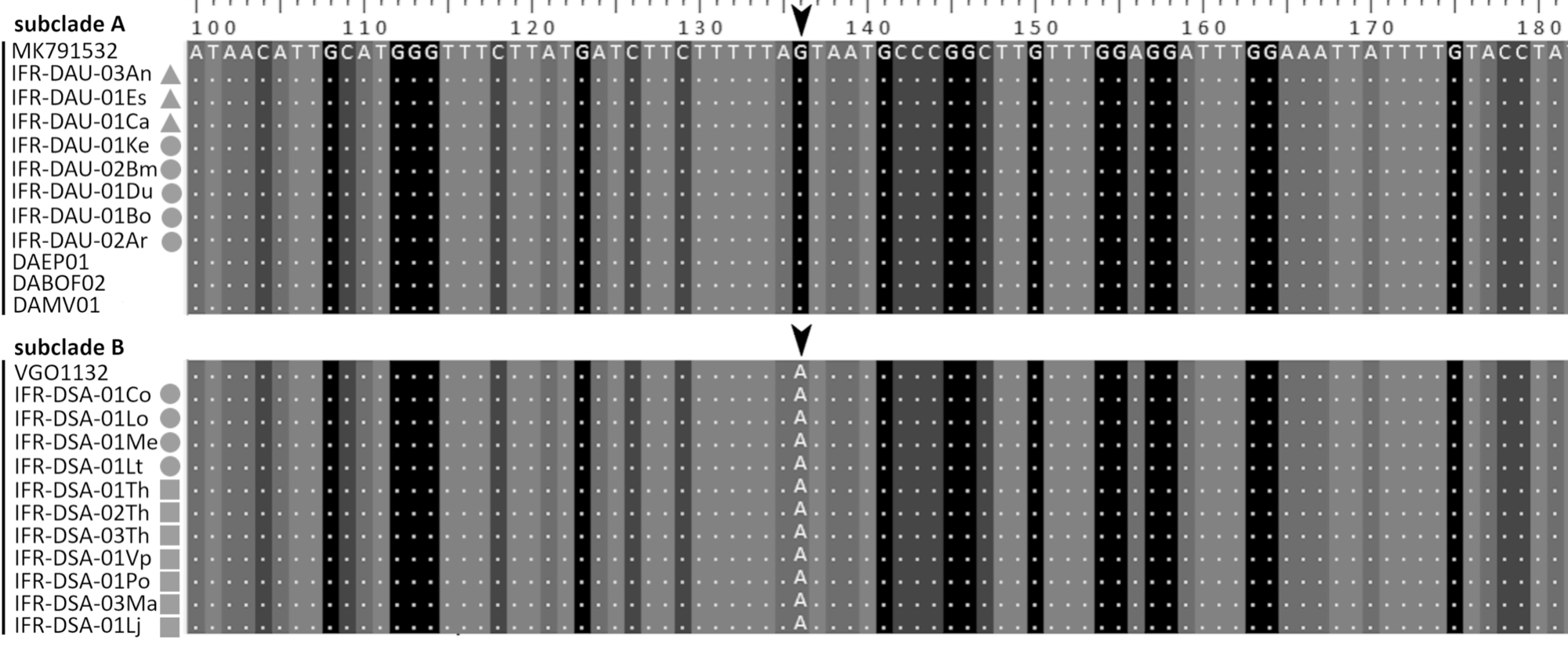
subclade A
100
110
120
130
140
150
160
170
180
MK791532
ATAACATTGCATGGGTTTCTTATGATCTTCTTTTTAGTAATGCCCGGCTTGTTTGGAGGATTTGGAAATTATTTTGTACCTA
IFR-DAU-03An
IFR-DAU-01Es
IFR-DAU-01Ca
IFR-DAU-01Ke
IFR-DAU-02Bm
IFR-DAU-01Du
IFR-DAU-01Bo
IFR-DAU-02Ar
DAEP01
DABOF02
DAMV01
subclade B
VGO1132
IFR-DSA-01Co
IFR-DSA-01Lo
IFR-DSA-01Me
IFR-DSA-01Lt
IFR-DSA-01Th
IFR-DSA-02Th
IFR-DSA-03Th
IFR-DSA-01Vp
IFR-DSA-01Po
IFR-DSA-03Ma
IFR-DSA-01Lj
A

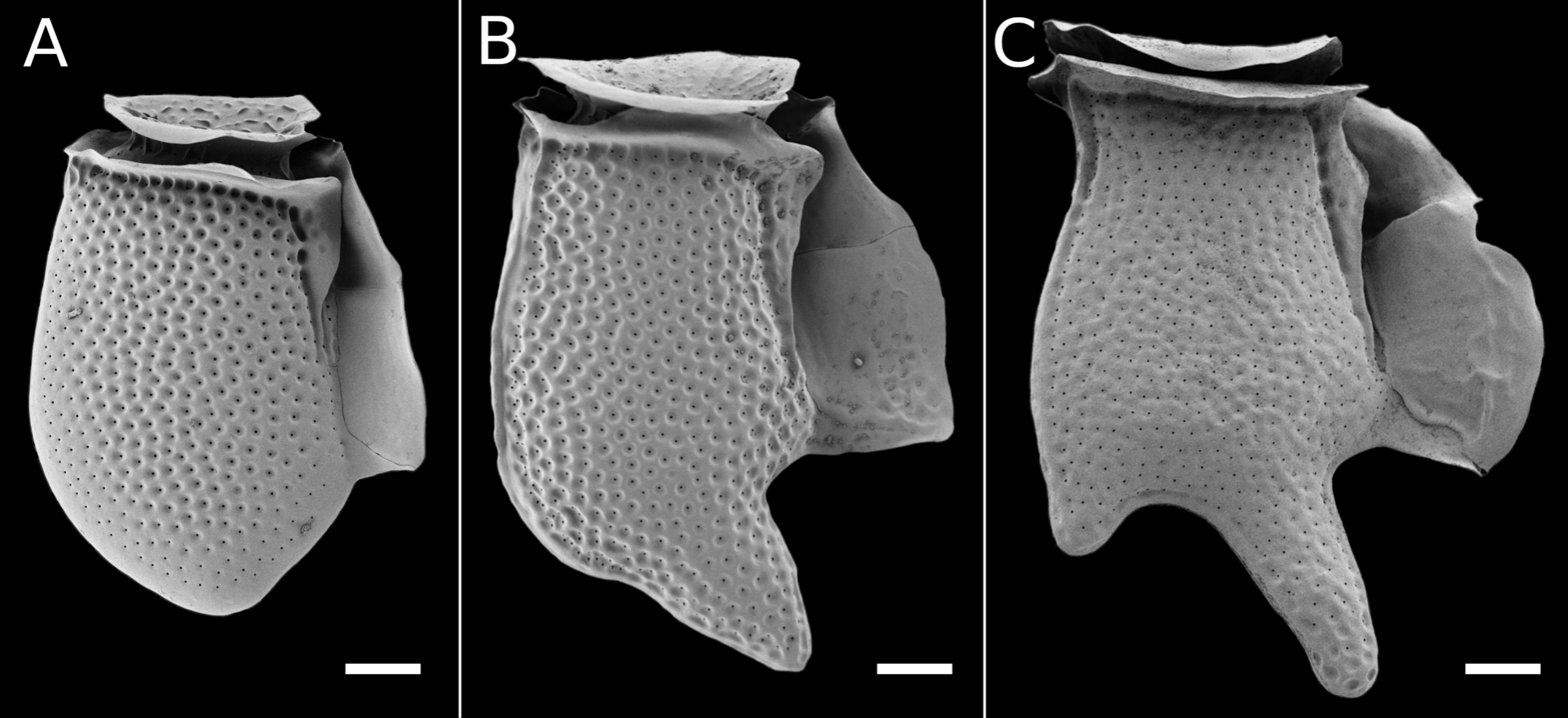
A
B
C

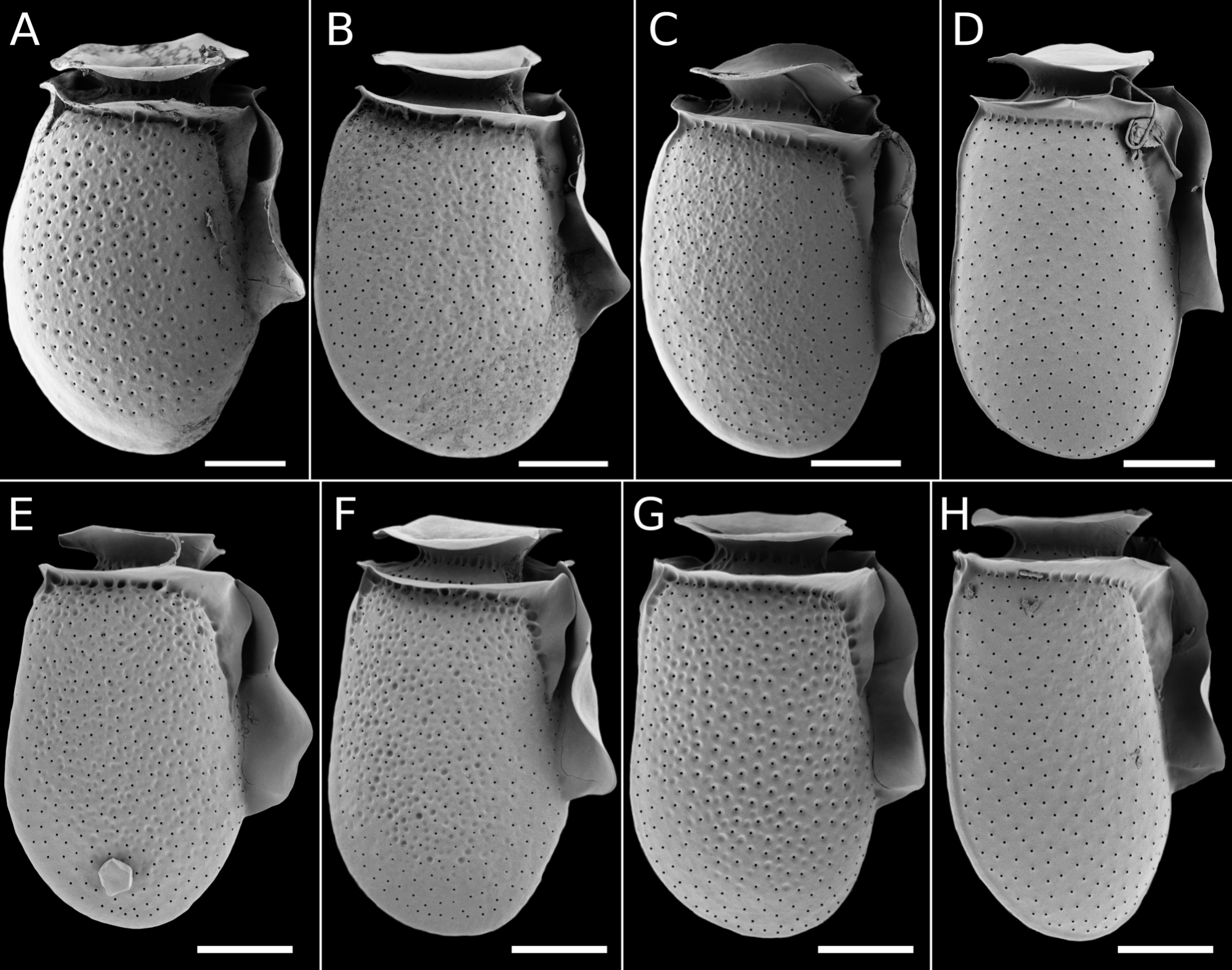
A
B
C
D
E
F
G
H

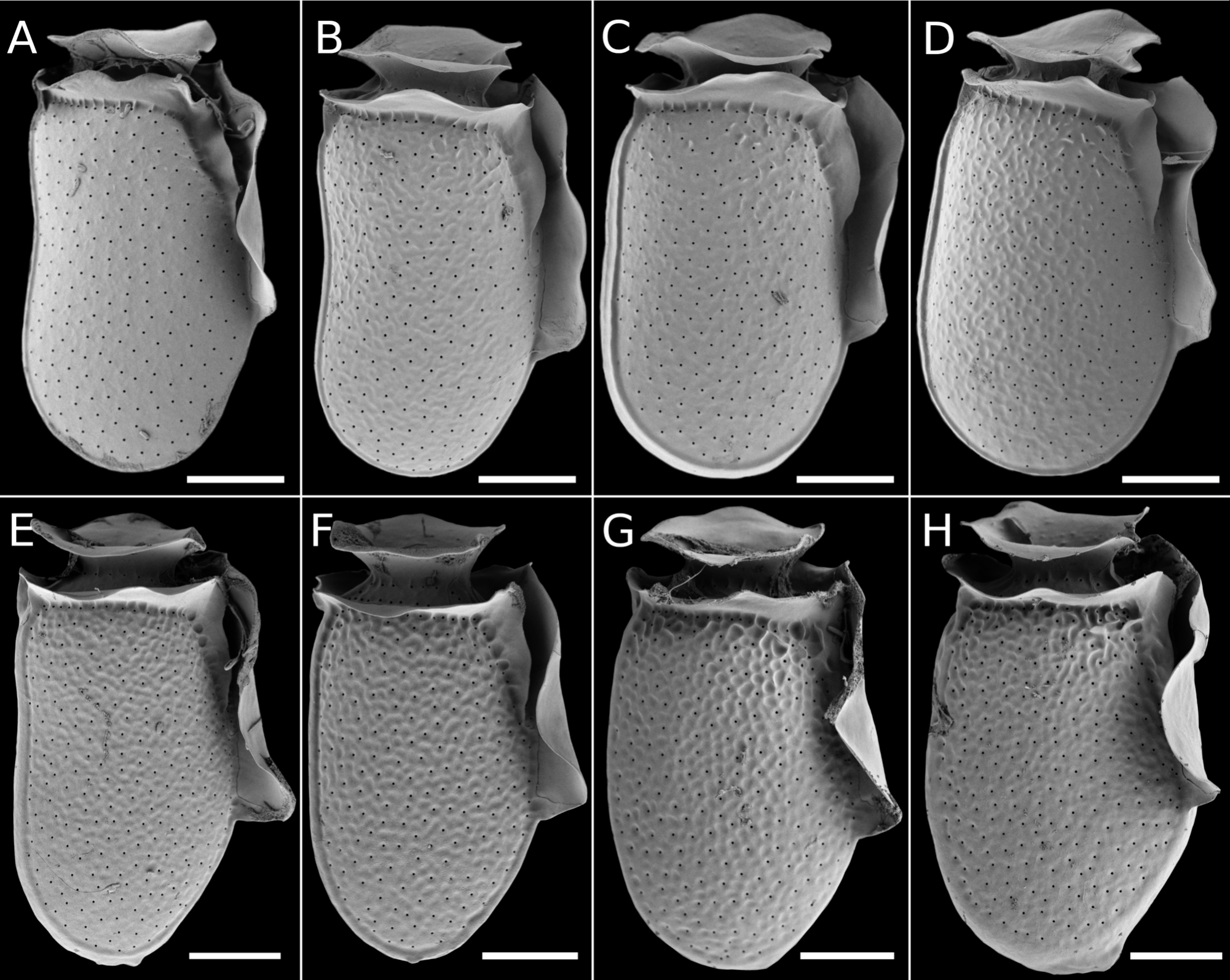
A
B
C
D
E
F
G
H

Table 1. List of the thirty strains of *Dinophysis* sp isolated from French coast during this study

Strain	Species	Collection date	Origin	Coordinates	GenBank accession # LSU	*cox1*	Toxin present AO	C9-diol OA	DTX2	PTX2
IFR-DAU-03An	*D. acuminata* complex	Aug-19	Antifer	49.66575N 0.131659E	MT365093	MT371856	+	<LOD	<LOD	<LOD
IFR-DAU-01Es	*D. acuminata* complex	Aug-19	Saint Aubin - les Essarts	49.36424N 0.38901W	MT365094	MT371857	+	<LOD	<LOD	<LOD
IFR-DAU-01Ca	*D. acuminata* complex	Aug-19	Cabourg	49.29840N 0.11700W	MT365095	MT371858	+	<LOD	<LOD	<LOD
IFR-DAU-01Ke	*D. acuminata* complex	May-18	Kervel	48.11279N 4.29085W	MT365096	MT371859	+	<LOD	<LOD	<LOD
IFR-DAU-01Du	*D. acuminata* complex	Oct-17	Dumet	47.42272N 2.59545W	MT365097	MT371860	+	<LOD	<LOD	<LOD
IFR-DAU-02Bm	*D. acuminata* complex	Apr-19	Le Croisic	47.22916N 2.58333W	MT365098	MT371861	+	<LOD	<LOD	<LOD
IFR-DAU-01Bo	*D. acuminata* complex	Apr-19	Noirmoutier	47.01908N 2.199944W	MT365099	MT371862	+	<LOD	<LOD	<LOD
IFR-DAU-02Ar	*D. acuminata* complex	May-18	Arcachon	44.54228N 1.26374W	MT365100	MT371863	+	<LOD	<LOD	<LOD
IFR-DSA-01Co	*D. acuminata* complex	Jul-19	Concarneau	47.83341N 3.94992W	MT365101	MT371864	+	<LOD	<LOD	+
IFR-DSA-01Lo	*D. acuminata* complex	May-16	Loscolo	47.40275N 2.73007W	MT365102	MT371865	+	+	<LOD	+
IFR-DSA-01Me	*D. acuminata* complex	May-15	Arcachon	44.64769N 1.10039W	MT365103	MT371866	+	+	<LOD	+
IFR-DSA-01Lt	*D. acuminata* complex	May-15	La Teste de Buch	44.64589N 1.14531W	MT365104	MT371867	+	+	<LOD	+
IFR-DSA-01Th	*D. acuminata* complex	Dec-15	Thau Lagoon	43.44731N 3.67054E	MT365105	MT371868	+	+	<LOD	+
IFR-DSA-02Th	*D. acuminata* complex	Oct-17	Thau Lagoon	43.44731N 3.67054E	MT365106	MT371869	+	+	<LOD	+
IFR-DSA-03Th	*D. acuminata*	Mar-18	Thau Lagoon	43.44731N	MT365107	MT371870	+	<LOD	<LOD	+

	complex			3.67054E						
	D. acuminata			43.49147N						
IFR-DSA-01Vp	complex	Mar-18	Vic Lagoon	3.82587E	MT365108	MT371871	+	<LOD	<LOD	+
	D. acuminata			43.55907N						
IFR-DSA-01Po	complex	Mar-18	Ponant Lagoon	4.10167E	MT365109	MT371872	+	<LOD	<LOD	+
	D. acuminata			43.46871N						
IFR-DSA-01Ma	complex	Mar-18	Berre Lagoon	5.02094E	MT365110	MT371873	+	+	<LOD	+
	D. acuminata			43.40813N						
IFR-DSA-01Lj	complex	Mar-18	Berre Lagoon	5.15436E	MT365111	MT371874	+	+	<LOD	+
				44.54228N						
IFR-DTR-01Ar	*D. tripos*	Apr-19	Arcachon	1.26374W	MT365115	MT371875	<LOD	<LOD	<LOD	+
				48.11279N						
IFR-DCA-01Ke	*D. caudata*	Oct-17	Kervel	4.29085W	–	–	<LOD	<LOD	<LOD	+
				48.11279N						
IFR-DCA-03Ke	*D. caudata*	Oct-17	Kervel	4.29085W	–	–	<LOD	<LOD	<LOD	+
				47.40275N						
IFR-DCA-02Lo	*D. caudata*	Oct-17	Loscolo	2.73007W	–	–	<LOD	<LOD	<LOD	+
			Grand Travers							
			beach (La	43.55631N						
IFR-DCA-04Tr	*D. caudata*	Aug-19	Grande Motte)	4.03588E	MT365116	MT371876	<LOD	<LOD	<LOD	+
				48.11279N						
IFR-DAC-03Ke	*D. acuta*	Nov-17	Kervel	4.29085W	MT365112	MT371877	+	<LOD	+	+
				47.30343N						
IFR-DAC-02Lc	*D. acuta*	Aug-17	Le Croisic	2.53849W	MT365113	MT371878	+	<LOD	+	+
				47.30343N						
IFR-DAC-03Lc	*D. acuta*	Aug-17	Le Croisic	2.53849W	–	–	+	<LOD	+	+
				47.30343N						
IFR-DAC-04Lc	*D. acuta*	Oct-17	Le Croisic	2.53849W	–	–	+	<LOD	+	+
				44.54228N						
IFR-DAC-01Ar	*D. acuta*	Aug-17	Arcachon	1.26374W	MT365114	MT371879	+	<LOD	+	+
				43.55907N						
IFR-DAC-01Po	*D. acuta*	Jul-18	Ponant Lagoon	4.10167E	–	–	+	<LOD	+	+

Table 2. Primers used for DNA amplification in the two rounds of the semi-nested/nested PCR

Primer	Sequence (5′-3′)	PCR rounds	Reference
ITSFW	GTA GGT GAA CCT GCG GAA GG	1, 2	Adam et al., 2000
D3B	TCG GAG GGA ACC AGC TAC TA	1	Nunn et al., 1996
D2C	CCT TGG TCC GTG TTT CAA GA	2	Scholin et al., 1994
Dinocox1F	AAA AAT TGT AAT CAT AAA CGC TTA GG	1, 2	Lin et al., 2002
Dinocox1R	TGT TGA GCC ACC TAT AGT AAA CAT TA	1	Lin et al., 2002
Cox777R	CAT TGA TTG GTT CSC AAA GA	2	This study

Table 3. Settings of mass spectrometric parameters (collision energy (CE); exit potential (CXP)), MRM transitions monitored in API 4000QTrap instrument (SCIEX, CA, USA) and the limits of detection (LOD) and quantification (LOQ) for the standards available.

Group	Source settings	Toxin	MRM transitions (*m/z*)	CE (eV)	CXP (eV)	LOD (ng mL^{-1})	LOQ (ng mL^{-1})
OA diol ester	Mode **ESI^+** CUR (psi) 30 TEMP (°C) 500 GS1 (psi) 50 GS2 (psi) 50 IS (V) 5500 DP (V) 66	C9-diol OA	965.4/827.4*	50	11		
			965.4/723.4	62	16		
		C9-triol OA	981.4/827.4*	50	11		
			981.4/723.4	62	16		
		C8-diol OA	946.6/805.6*	17	22	1.5	4
			946.6/751.6	35	20		
			946.6/787.6	21	20		
		C7-diol OA	937.4/827.4*	50	11		
			937.4/723.4	62	16		
		C6-diol OA	923.4/827.4*	50	11		
			923.4/723.4	62	16		
		C4-diol OA	897.4/827.4*	50	11		
			897.4/723.4	62	16		
OA and DTXs	Mode **ESI^-** CUR (psi) 25 TEMP (°C) 600 GS1 (psi) 40 GS2 (psi) 60 IS (V) -4500 DP (V) -170	AO, DTX2	803.4/255.1*	-62	-16	1	3
			803.4/113.1	-92	-9		
		DTX1	817.3/255.4*	-64	-9	1	3
			817.3/113.2	-92	-10		
PTXs	Mode **ESI^+** CUR (psi) 30 TEMP (°C) 450 GS1 (psi) 50 GS2 (psi) 50 IS (V) 5500 DP (V) 91	PTX2	876.6/823.5*	31	12	0.2	0.6
			876.6/805.6	37	12		
			876.6/213.6	55	12		
		PTX2sa *7-epi-*PTX2sa	894.6/823.5*	31	12		
			894.5/805.5	37	12		
			894.5/213.6	55	12		
		PTX1 PTX4 PTX11 PTX13	892.6/821.4	37	12		
			892.6/839.5*	31	12		
			892.6/213.6	55	12		
		PTX6 PTX7	906.6/871.6*	31	12		
			906.6/853.6	37	12		
		PTX12 PTX14	874.5/839.6*	31	12		
			874.6/213.6	55	12		

***MRM transition used for quantification in each method**

Table 4. Morphometric data and growth rates of 8 strains of the different species

Strain	Species	Length (mean ± s.d.) µm	Depth (mean ± s.d.) µm	L/D	*n*	µ (mean, range) Day^{-1}
IFR-DAU-03An	*D. acuminata*-complex	45.6 ± 2.3	31.3 ± 1.9	1.35–1.67	25	ND
IFR-DAU-01Ke	*D. acuminata*-complex	49.9 ± 3.6	33.6 ± 2.6	1.30–1.71	24	ND
IFR-DAU-02Ar	*D. acuminata*-complex	45.5 ± 5.3	29.6 ± 4.1	1.23–1.79	21	0.41, 0.40- 0.42
IFR-DSA-01Lt	*D. acuminata*-complex	45.4 ± 2.5	28.7 ± 2.7	1.38–1.86	25	0.43, 0.42- 0.44
IFR-DSA-02Th	*D. acuminata*-complex	46.5 ± 3.1	30.4 ± 1.8	1.36–1.66	25	ND
IFR-DAC-01Ar	*D. acuta*	67.1 ± 2.0	46.4 ± 2.7	1.33–1.63	25	0.23, 0.21- 0.26
IFR-DCA-04Tr	*D. caudata*	81.8 ± 2.4	43.3 ± 1.9	1.75–2.03	26	0.20, 0.19- 0.21
IFR-DTR-01Ar	*D. tripos*	97.6 ± 3.0	48.7 ± 3.3	1.78–2.37	25	0.22, 0.21- 0.24

Table 5.Summary of the toxin profiles of *D.acuminata*-complex (mitochondrial gene cox1 identified) from this study and literature

Strain	Origin	Subclade	OA	DTX1	PTX2	Reference
IFR-DAU-03An	France	A	+	<LOD	<LOD	Present study
IFR-DAU-01Es	France	A	+	<LOD	<LOD	Present study
IFR-DAU-01Ca	France	A	+	<LOD	<LOD	Present study
IFR-DAU-01Ke	France	A	+	<LOD	<LOD	Present study
IFR-DAU-02Bm	France	A	+	<LOD	<LOD	Present study
IFR-DAU-01Du	France	A	+	<LOD	<LOD	Present study
IFR-DAU-01Bo	France	A	+	<LOD	<LOD	Present study
IFR-DAU-02Ar	France	A	+	<LOD	<LOD	Present study
DAEP01	USA	A	+	+	+	Tong et al. 2015
DABOF02	Canada	A	<LOD	<LOQ	+	Tong et al. 2015
DAMV01	USA	A	+	+	+	Tong et al. 2015
VGO1132	Spain	B	+	+	+	Riobò et al. 2013 Raho et al. 2013
IFR-DSA-01Co	France	B	+	<LOD	+	Present study
IFR-DSA-01Lo	France	B	+	<LOD	+	Present study
IFR-DSA-01Me	France	B	+	<LOD	+	Present study
IFR-DSA-01Lt	France	B	+	<LOD	+	Present study
IFR-DSA-01Th	France	B	+	<LOD	+	Present study
IFR-DSA-02Th	France	B	+	<LOD	+	Present study
IFR-DSA-03Th	France	B	+	<LOD	+	Present study
IFR-DSA-01Vp	France	B	+	<LOD	+	Present study
IFR-DSA-01Po	France	B	+	<LOD	+	Present study
IFR-DSA-01Ma	France	B	+	<LOD	+	Present study
IFR-DSA-01Lj	France	B	+	<LOD	+	Present study